On the links between meteorological variables, aerosols, and tropical cyclone frequency in individual ocean basins

Marc Chiacchio[1,2], Francesco S. R. Pausata[1,2], Gabriele Messori[1,2], Abdel Hannachi[1], Mian Chin[3], Thomas Önskog[4], Annica M. L. Ekman[1,2], Leonard Barrie[1,2]

[1]Department of Meteorology, Stockholm University, Stockholm, Sweden
[2]Bert Bolin Centre for Climate Research, Stockholm, Sweden
[3]NASA Goddard Space Flight Center, Greenbelt, Maryland, USA
[4]Department of Mathematics, KTH, Stockholm, Sweden

Corresponding Author:
Marc Chiacchio
Department of Meteorology
Stockholm University
S-10691 Stockholm, Sweden
Email: marc.chiacchio@misu.su.se
Phone: +46 (0)8 16 2534

Key points

Significant impact of black carbon and organic aerosols

Significant impact of observed dust aerosols in the North Atlantic

Lower stratospheric temperatures explain 28% of the log-likelihood

This article has been accepted for publication and undergone full peer review but has not been through the copyediting, typesetting, pagination and proofreading process which may lead to differences between this version and the Version of Record. Please cite this article as doi: 10.1002/2015JD024593

Abstract

A generalized linear model based on Poisson regression has been used to assess the impact of environmental variables modulating tropical cyclone frequency in six main cyclone development areas: the East Pacific, West Pacific, North Atlantic, North Indian, South Indian, and South Pacific. The analysis covers the period 1980-2009 and focuses on widely used meteorological parameters including wind shear, sea surface temperature, and relative humidity from different reanalyses as well as aerosol optical depth for different compounds simulated by the GOCART model. Circulation indices are also included. Cyclone frequency is obtained from the International Best Track Archive for Climate Stewardship. A strong link is found between cyclone frequency and the relative sea surface temperature, Atlantic Meridional Mode, and wind shear with significant explained log-likelihoods in the North Atlantic of 37%, 27%, and 28%, respectively. A significant impact of black carbon and organic aerosols on cyclone frequency is found over the North Indian Ocean, with explained log-likelihoods of 27%. A weaker but still significant impact is found for observed dust aerosols in the North Atlantic with an explained log-likelihood of 11%. Changes in lower stratospheric temperatures explain 28% of the log-likelihood in the North Atlantic. Lower stratospheric temperatures from a subset of CMIP5 models properly simulate the warming and subsequent cooling of the lower stratosphere that follows a volcanic eruption but underestimate the cooling by about 0.5 °C.

1. Introduction

Tropical cyclone (TC) activity, frequency and intensity, varies on interannual and interdecadal timescales (e.g. Klotzbach, 2006; Landsea et al., 2006; Kossin et al., 2007; Klotzback and Gray, 2008; Kossin et al., 2013), but finding a robust theory to explain these fluctuations has proved challenging. A first major issue is the limited availability of accurate long-term TC records. The records typically have a limited temporal coverage (Knutson et al., 2010) and suffer from changes in technology and methodology (e.g., Nicholls et al., 1997a). The latter cause temporal heterogeneities and lead to errors such as spurious trends in the Pacific (Kunkel et al., 2013) and an underestimation of the number of extreme TCs in the North Indian Ocean (Landsea et al., 2006).

The role of natural climate variability in influencing TC activity has been studied in detail in the past, mainly using statistical methods (e.g. Nicholls, 1984; Gray 1984a,b; Evans and Allan, 1992; Dong and Holland, 1994; Landsea et al., 1999), global (e.g. Ouuchi et al., 2006; Bengtsson et al., 2007; Knutson et al., 2010; Murakami et al., 2012; Camargo, 2013) and regional (e.g. Diro et al., 2014) climate modeling. These and other studies (e.g. Emanuel and Nolan, 2004; Camargo et al., 2007; Tippett et al., 2011) have proposed many environmental variables as proxies or genesis potential indices for TC activity. Amongst them are sea surface temperature (SST), lower to middle level relative humidity (RH), and modes of general circulation of the atmosphere including the quasi-biennial oscillation (QBO), El Niño-Southern Oscillation (ENSO), the Atlantic Multidecadal Oscillation (AMO), and the Atlantic Meridional Mode (AMM).

The role of ENSO in modulating TC variability has received significant attention (e.g. Camargo et al., 2005; Wang et al., 2014). SST anomalies are the main thermodynamic contributor by which ENSO influences TC activity (e.g. Gray, 1984; Elsner et al., 2001), while wind shear is the main dynamical factor (Wang and Lee, 2009). In the North Atlantic, the latter was found to be more important than ENSO-related thermodynamic effects (Camargo et al., 2007). During an ENSO warm phase – El Niño – an increase in upper tropospheric westerly winds (Wang and Lee, 2009) in the North Atlantic region enhances the vertical wind shear; this then inhibits the formation and further development of TCs in the North Atlantic and facilitates those in the East Pacific. The opposite occurs during the ENSO cold phase – La Niña – where an increase in TCs is observed in the North Atlantic while a decrease is observed in the East Pacific. Other studies addressed teleconnection patterns, finding an increase in TC frequency in the western North Pacific during strong El Niño events and a shift in TC genesis to the southeast of this region during an El Niño and to the northwest during a La Niña (Wang and Chan, 2002, Camargo and Sobel, 2005). There is also evidence for increased hurricane numbers in the central and eastern North Pacific region during an El Niño (e.g. Frank and Young, 2007; Grey and Sheaffer, 1991). In the North Indian Ocean basin, fewer intense TCs occurred during El Niño events (Sing et al., 2000) while in the South Indian Ocean there were a greater number of TCs during La Niñas (Kuleshov and de Hoedt, 2003). There have also been a number of studies conducted in the South Pacific and Australian basins (e.g. Nicholls, 1979; Basher and Zeng, 1995), which found an increase in the number of TCs in the southwest Pacific during El Niño years. Specifically, TC genesis regions in these basins shift eastward (El Niño) and westward (La Niña) (Evans and Allen, 1992; Camargo et al., 2007) as well as northward (El Niño) and southward (La Niña) (Revell and Goulter, 1986; Camargo et al., 2007). Finally, ENSO has also been proposed as the underlying factor for the inverse relationship observed between the

North Atlantic and East Pacific TC frequencies (Landsea and Gray, 1989; Collins, 2007, 2010, and Tang and Neelin, 2004).

Analogous studies have addressed the interaction of other climate modes with TCs. Gray (1984a; b) was the first to propose that the westerly phase of the QBO corresponds to an increased TC activity in the North Atlantic while the easterly phase of the QBO is associated with a decrease in TC activity in the West Pacific. However, more recently Camargo and Sobel (2010) show that such a relationship is not found after the 1980s, and a clear explanation for this change is still missing. The AMO has been linked to the intense hurricane season of 2005 over the Atlantic (Trenberth and Shea, 2006), and its strong dominance over climate variability has been shown to temporarily counteract the possible influence of global warming on TCs (Chylek and Lesins, 2008). Related to the AMO is the AMM, which describes the meridional variability in the tropical Atlantic Ocean. The AMM has been found to be strongly linked to seasonal hurricane activity on both interannual and decadal time scales. Thus, it reinforces the argument for a strong dynamical relationship between the climate and TC activity (Tang and Neelin, 2004; Vimont and Kossin, 2007).

In addition to the traditional tropospheric drivers of TC variability, some studies have investigated the influence of the stratosphere. Stratospheric forcing can directly influence both upper and lower-tropospheric dynamics (for a comprehensive review see Song and Robinson, 2004), and there is also evidence that the stratosphere affects synoptic structures in the tropical regions. Thus, it is reasonable to assume that their influence extends to TCs. A number of studies have linked stratospheric winds to cyclone frequency (*e.g.* Gray, 1984a; Chan, 1995). The proposed physical connection is that the westerlies in the lower stratosphere affect vertical wind shear in the upper troposphere, thus favoring or suppressing

the formation of TCs. More recent studies have highlighted the influence of stratospheric temperature anomalies on the potential intensity of cyclones (Emanuel et al., 2013; Vecchi et al., 2013). The temperature of the lower stratosphere affects the cyclone's outflow temperature, which is one of the factors determining the cyclone's thermal efficiency. The TC's thermal efficiency is directly related to the ratio of SST and outflow temperature, whereby a colder stratosphere will lead to a colder outflow temperature, hence raising thermal efficiency (Ramsay, 2013). However, all of these studies have only analyzed the link between stratospheric temperatures and TC intensity, without considering possible impacts on frequency.

The role of anthropogenic climate forcing in affecting TC activity is even harder to quantify than that linked to natural fluctuations, and large uncertainties still exist (Mann and Emanuel, 2006; Knutson et al., 2010). The problem is intrinsically complex, since it requires detecting the net effect of multiple small drivers on a system with a large background noise. For instance, increased surface temperature due to global warming is expected to also lead to increased potential intensity of TCs as first investigated in Emanuel (1987) and Holland (1997) and heighten the probability of more intense TCs occurring in the future (Emanuel 1987, 2013; Bengtsson et al., 2007; Knutson et al., 2010, Murakami et al., 2012). On the other hand, local surface cooling due to natural and anthropogenic aerosols will likely suppress their development (Mann and Emanuel, 2006; Evan et al., 2006a; Evan et al., 2012; Dunstone et al., 2013; Wang et al., 2014), and assessing the two effects separately is no easy task. There is evidence that aerosols have influenced multidecadal changes in SST by modifying the net surface shortwave radiation (Booth et al., 2012), but further work is necessary to assess the degree of this forcing on SST variability (Zhang et al., 2012). Indeed, the potential influence of short-lived anthropogenic aerosols on TC activity is only beginning

to be explored. Associating trends in TCs with climate change is therefore challenging, and recent efforts to study the influence of natural variability versus anthropogenic forcing on TC activity (e.g. Emanuel and Mann, 2006; Ting et al., 2015) have obtained conflicting results.

Notwithstanding the vast literature reviewed here, there is no clear overview and comparison of the dependence of TC frequency on external variables in all six major TC regions of the globe. The aim of this study is to fill this gap by analyzing the fraction of explained deviance or fraction of explained log-likelihood associated with the observed meteorological and environmental variables in each basin, and by discussing the results in terms of the underlying physical processes that are likely to drive TC activity. Throughout the analysis we adopt a statistical linear model based on Poisson regression. Unlike previous studies, all six major oceanic regions displaying TC development are considered: the East Pacific (EP), West Pacific (WP), North Atlantic (NA), North Indian (NI), South Indian (SI), and South Pacific (SP) (see Figure 1 for their geographical location and Table 1 for their coordinates). The complete list of variables we investigate is provided in Table 2. Because of the limited reanalysis time series of 30 years we do not include the AMO, which is found to be uncorrelated to TC activity on interannual time scales (Vimont and Kossin, 2007). We further use relative SSTs, in addition to absolute values. As noted in Vecchi and Soden (2007, 2008), Swanson (2008) and Camargo et al. (2013), the relative warming of the local SST with respect to the warming of the tropics is the variable that more strongly modifies TC potential intensity. While we focus on TC frequency rather than intensity, we nonetheless decide to investigate relative SSTs for coherence with the literature. Some of the variables analyzed here, such as lower (1000-850 hPa) and middle (700-500 hPa) level RH, SST and ENSO, have been commonly used in tropical cyclone research, albeit over more limited geographical

domains. Other variables have generally not been extensively studied in the past. These include:

i) Aerosol optical depth of several atmospheric components including: black and organic carbon (BC and OC, respectively), sulfate (SU), dust (DU), and sea salt (SS). There is only a limited amount of research suggesting a possible influence of these variables on climate and on tropical cyclones in particular (e.g., Emanuel and Mann, 2006; IPCC AR5 report, Wang et al 2012; Dunstone et al, 2013)

ii) Lower stratospheric temperature at 100 hPa, motivated by Emanuel's (2013) theory that lower stratospheric cooling influenced the recent TC potential intensity changes.

Where possible, the results are compared to the existing literature and tested for self-consistency. The statistical relationships we find between observed variables and TC frequency can be useful in testing the performance of climate models.

Section 2 provides a detailed overview of the datasets used and the methodology; Section 3 presents the results of the regression analysis linking the tropospheric and lower-stratospheric variables to TC frequency in the different basins. Section 4 discusses the results in terms of physical processes and section 5 provides a summary and conclusions.

2. Data and Methodology

2.1 TC Domains

The analysis considers the six main oceanic regions displaying TC development. The choice of the NA region was based on the "Main Development Region" (MDR) defined in Goldenberg and Shapiro (1996), while the EP region of development was taken from Collins (2010). To our knowledge, there are no widely used conventions for the regions of TC development in the other areas we address. We have therefore defined these regions according to the IBTrACS storm tracks presented in Figure 3a of Knapp et al. (2010). Note that no land grid boxes are considered in the above domains. We have calculated the seasonal and five-year running mean TC frequency in each ocean basin for the period 1980-2009 (Figure 2). The values for each basin are computed over the period of strongest TC activity as defined in Table 1.

2.2 The Datasets

The present study uses data from a wide range of analysis products based on observations and in the case of aerosols, on chemical transport modeling and historical global emissions evaluated with remote sensing observations. The TC tracks are obtained from the National Oceanic and Atmospheric Administration's (NOAA) IBTraCS dataset (v03r05, Knapp et al., 2010; Kruk et al., 2010). This enables us to compare the TC frequency in the different basins. The dataset covers the period 1842-2012, and we select 1980 as the start of our time series because prior data are less reliable (Landsea et al., 2004; Trenberth and Shea, 2006).

Most of the climatic variables analyzed (see Table 2) are obtained from the European Centre for Medium-Range Weather Forecasts' (ECMWF) ERA-Interim reanalysis (Dee et al., 2011), the Modern-Era Retrospective Analysis for Research and Applications (MERRA) (Rienecker et al., 2011), and the National Centers for Environmental Research/National Center for Atmospheric Research (NCEP/NCAR) reanalysis project (Kalnay et al., 1996). Only the period since 1980, when satellite assimilation began, is considered here. The vertical wind shear is calculated as the difference between zonal winds at 200 and 850 hPa, as commonly defined in the literature (e.g. Goldenberg et al., 2001; Zhang and Delworth, 2006; Ng and Chan, 2012). The relative SST is computed as the difference between the local SST, (i.e. SST averaged over the MDR or any of the other TC development regions as defined in Table 1) and the average SST of the tropical ocean basins from 20° North to 20° South. ERA-Interim has a horizontal resolution of 80 km and 60 vertical levels from the surface to 0.1 hPa.

Based upon previous work (e.g. Murakami, 2014), TC distribution and seasonal variation of reanalyses, which includes all those in our study, compare well with observations even when using a different TC detection algorithm. There were also statistically significant correlations found, especially in the western North Pacific and North Atlantic basins, between the observed and detected interannual variability of the TC genesis number. From these results, we point out that the reanalyses we used provide a coherent representation of TC climatology.

The atmospheric aerosol optical depth (AOD) values come from simulations using the Goddard Chemistry Aerosol Radiation and Transport (GOCART) model, which considers the aerosol compounds of BC, OC, SU, DU, and SS according to Chin et al. (2002, 2014). GOCART uses prescribed meteorological fields from MERRA over the period 1980-2009, with a spatial resolution of 2º latitude × 2.5º longitude and 72 vertical levels extending from the surface to 0.01 hPa (Chin et al., 2014). The calculation of the AOD is performed at 550 nm and is based on the aerosol mass and optical properties from the Global Aerosol Data Set (GADS) (Köpke et al., 1997; Chin et al, 2002), updated for non-spherical dust particle properties (Chin et al., 2014). Modeled results of the global AOD distributions have been compared extensively to satellite and station data in Chin et al. (2014), including over the oceans. The model is able to capture the main patterns of AOD change found in satellite data such as the declining aerosols level over Europe due to stricter air pollution emission control enforced starting in the mid-1980s and the increase of combustion aerosols over Asia. Another robust feature found is the reduction of AOD between the late 1980s and the late 2000s (see Figure 11 in Chin et al., 2014) of dust aerosol outflow over the tropical North Atlantic, which agrees with the available satellite data and surface dust concentration observations. We therefore deem the dataset appropriate for the present study. Additional information on the GOCART simulations can be found in Chin et al. (2014).

In addition to the modeled dust AOD, observed dust AOD was also obtained from a dataset where a dust retrieval algorithm was applied using data from the Advanced Very High Resolution Radiometer (AVHRR) instrument onboard polar orbiting satellites (Evan and Mukhopadhyay, 2010). The algorithm is an advanced method that improves the ability to discern dust from clouds even during dust storms when the dust is optically thick from dust storms. The monthly mean dust AOD was retrieved over the northern tropical Atlantic (0-30°

N, 10-65° W) with a 1° × 1° horizontal resolution and as a monthly mean over the period January 1982-May 2010. We then compare the impact of observed dust AOD versus modeled (i.e. GOCART) dust AOD on TC frequency in the NA. The temporal correlation between the modeled and observed dust AOD in the NA is 0.8.

The stratospheric aerosol optical depth (SAOD) is estimated using solar occultation from the Stratospheric Aerosol Monitor (SAM) II and Stratospheric Aerosol and Gas Experiment (SAGE) II satellites. The data were obtained from NASA Goddard Institute for Space Studies (GISS, Sato et al., 1993). The SAOD is currently available from 1850-2012 as a zonal mean over 8º latitude bands, ranging from 90°N to 90°S. Due to the coarse meridional resolution of the data, the SAOD averages for the individual basins do not always match the exact northern and southern domains shown in Figure 1. We limit our analysis to the period 1980-2009 to match the temporal coverage of the GOCART AODs and to utilize the period when satellite data have greatly increased the number of available observations.

Part of the analysis focuses on the role of lower stratospheric cooling in affecting TC activity. To analyze such cooling, we used a multi-model mean (MMM) from the Coupled Model Intercomparison Project Phase 5 (CMIP5) simulations, for the period 1950-2005. The MMM includes CCSM4, CNRM-CM5, GFDL-CM3, GISS-E2-R, and NorESM1-M (see Table 3). These models were chosen because they include the full radiative effects of volcanic aerosols and interactive or semi-offline stratospheric ozone chemistry.

Finally, the analysis also considers several modes of atmospheric circulation, namely the AMM, ENSO, North Atlantic Oscillation (NAO), and QBO. We decided not to include the Arctic Oscillation as it is highly correlated to the NAO (Ambaum et al., 2001; Hannachi et al., 2009). The AMM index is based on the maximum covariance analysis of SSTs and the zonal and meridional components of the 10 m winds with the seasonal cycle removed. The data are also detrended and a three-month running mean applied following Chiang and Vimont (2004). The ENSO index used here is the "Multivariate" ENSO Index (MEI), based on sea-level pressure and SSTs in the tropical Pacific. The index is calculated from the first principal component (PC) of these two variables, taken from the UK Met Office Hadley Centre data (Wolter and Timlin, 2011). The NAO index is derived from the first PC of monthly-mean 700 hPa geopotential heights, and was taken from the NOAA Climate Prediction Center, following Barnston and Livezey (1987). The QBO is the zonal average of the 30 hPa zonal wind at the equator, as calculated by the NOAA Earth System Research Laboratory.

All indices and atmospheric variables are averaged over the TC seasonal periods displayed in Table 1, relative to the domains shown in Figure 1. This methodology is based on Sabbatelli and Mann's (2007) study of the NA's SSTs and TC counts.

2.3 Statistical Methods

The analysis is based on the statistical technique of Poisson regression, which is suitable for count data. Thus, we make the assumption that the conditional expectation of the dependent variable *Y* (i.e. the number of TCs in a given basin) with respect to a vector *x* containing the 18 variables considered in each basin (see Table 2 for a list) is given by:

$$E[Y|x] = exp(\alpha_0 + \sum_{i=1}^{18} \alpha_i x_i), \qquad (1)$$

where α_0 ,…, α_{18} are the regression coefficients. From the probability function of the Poisson distribution, we find that the conditional probability of observing *y* cyclones given the vector *x* of variables and the vector $\alpha = (\alpha_0, \ldots, \alpha_{18})$ of regression coefficients is:

$$p[y|x,\alpha] = \frac{e^{y\left(\alpha_0+\sum_{i=1}^{18}\alpha_i x_i\right)}e^{-e^{\alpha_0+\sum_{i=1}^{18}\alpha_i x_i}}}{y!}. \qquad (2)$$

Based on these conditional probabilities, we construct the likelihood function, which we maximize in order to find the optimal choice of α.

To quantify the influence of the different variables on the number of TCs in each basin, we let M_0 denote a constant Poisson regression model and M_i a Poisson regression model based only on the ith of the 18 variables, x_i. The deviances of these Poisson regression models are defined by

$$D(M_0) = -2\big(log(p[y|\alpha_0]) - log(p[y|saturated\ model])\big), \qquad (3)$$

$$D(M_i) = -2\big(log(p[y|x_i,\alpha_0,\alpha_i]) - log(p[y|saturated\ model])\big), \qquad (4)$$

where the saturated model has one parameter for every observation and hence fits the data perfectly. The contributions of the 18 variables are quantified by the pseudo-R^2 measure (Cameron and Windmeijer, 1996; Heinzl and Mittlbock, 2003)

$$R^2 = \frac{log(p[y|x_i,\alpha_0,\alpha_i]) - log(p[y|\alpha_0])}{log(p[y|saturated\ model]) - log(p[y|\alpha_0])} = 1 - \frac{D(M_i)}{D(M_0)}, \qquad (5)$$

which can be interpreted as the fraction of explained deviance or fraction of explained log-likelihood. Under the null hypothesis that M_0 is the true model, the difference between the deviances (i.e. likelihood ratio test) of the two models, $D(M_0)$-$D(M_i)$, follows an approximate chi-squared distribution with one degree of freedom. The contribution to the number of TCs from variable *i* in a given basin was assessed for statistical significance at the 5% level using

the quantiles of the chi-squared distribution. Since we are considering 18 statistical inferences simultaneously, the multiple testing problem arises. If the 18 variables are perfectly dependent, the overall significance level is obtained by using the 5% level in each of the tests, but if the variables are independent, the correct significance level to use in the individual tests is 0.05/18. The appropriate level clearly depends on the dependence and distribution of the variables, which are generally unknown. To address this issue, a significance level of 2.5% was used in all of the individual tests. Note that we only discuss pseudo-R^2 results that fall within this significance level unless otherwise stated. The significance of other results is computed at the 5% level (i.e., Figure 7).

3. Results

Here we focus on the fraction of explained log-likelihood (pseudo-R^2) and sign of the regression coefficients from the Poisson regression between TC frequency and climatic variables in each basin (Figure 3). Though we use meteorological variables from the MERRA, ERA-Interim, and NCEP datasets in the analysis, we only report our results dealing with the Poisson regression using MERRA. In fact, the latter dataset provides the most statistically significant regression results. Nonetheless, the other two datasets are in general agreement with MERRA, as can be seen in the Appendix. A similar analysis with variables mainly including circulation indices and SST was carried out in Sabbatelli and Mann (2007) and Caron et al. (2015) in the NA. We first examine the link between TC frequency and tropospheric (section 3.1) and stratospheric variables (section 3.2). Finally, we discuss TC frequency in relation with the circulation modes (section 3.3).

3.1 Tropospheric variables associated with TC frequency

3.1.1 SSTs and atmospheric variables

The relation between absolute SSTs and TCs shows pseudo-R^2 values close to or exceeding 22% in the EP, NA, SI and SP, indicating a large influence of SSTs on the frequency of TCs in these basins (Figure 3). In the WP and NI Oceans, the pseudo-R^2 values are not significant, in agreement with previous findings (e.g., Chan and Liu, 2004; Ng and Chan, 2012). Interestingly, the EP and NA both have significant positive regression coefficients, while SI and SP both have negative regression coefficients. The negative regression coefficients found in the SI and SP appear counterintuitive. Out of all the 18 variables analyzed, the relative SST dominates in the NA and SP with pseudo-R^2 values of 37% and 30%, respectively. Similarly to the SSTs, precipitable water can be regarded as a potential energy source through its release of latent heat for TC development (Vasquez, 1994), and explains a significant portion of TC variability in multiple basins: the NA, NI, SI, SP. The sign of the regression coefficients for the precipitable water is always positive in the NA and NI but is negative in the SI and SP.

RH is a variable often found to be linked with TCs, but the NA is the only basin where a statistically significant impact on TC frequency was found. The corresponding regression coefficient was negative and the pseudo-R^2 was 14%. The NA is also the only basin where wind shear is statistically significant with an explained log-likelihood of as much as 27%, in agreement with Aiyyer and Thorncroft (2011). As for RH, the wind shear also displays a negative regression coefficient. In the other basins, the TC frequency is dominated by either modes of variability or aerosols.

3.1.2 Tropospheric aerosols

The only significant positive link between TC frequency and aerosols is found for BC and OC in the NI (Figure 3d). The similar result for OC and BC is not surprising as combustion-derived BC and OC, in particular from biomass burning, have similar source distributions (e.g. Bond et al., 2007). There is no strong link with aerosol concentration/AOD elsewhere. In the NI Ocean (Figure 3d), the explained log-likelihoods of BC and OC are 27%. An increase in BC causes a heating in the lower troposphere from solar absorption, as well as a negative radiative forcing at the surface (Meywerk and Ramanathan, 1999). A negative surface forcing may in turn result in a decrease in the meridional SST gradient, and a weakening of the lower tropospheric tropical easterly jet (Chung and Ramanathan, 2006; Meehl et al., 2008; Evan et al., 2011). Evan et al. (2011) argued that this would weaken the monsoon circulation and reduce the strength of the vertical wind shear, ultimately promoting TC development and activity. Such a mechanism is in agreement with our finding. See Section 4.1 for more details.

For SS, the only significant results are found in the NA and SP (Figures 3c and 3f), with pseudo- R^2 values of 11% and 18% and with negative and positive regression coefficients, respectively. The large explained log-likelihood of SS in the SP is consistent with the finding that, during extreme weather, large sea-salt particles can lead to an intensification of TCs (Zhang and Perrie, 2006). It is also plausible that strong TC activity can lead to more sea-salt emission. Nonetheless, large amounts of sea spray generation can substantially change the transfer of energy from the ocean's surface to the atmosphere (Fairall et al., 1994), and increase the surface heat fluxes (i.e., latent and sensible heat exchange) during conditions of high winds and warmer SSTs (Zhang et al., 2006). In the NA, the significant impact of SS with a negative regression coefficient could be due to the dominant role of windshear, that is

negatively associated to TC frequency in this basin. Therefore, with a stronger windshear, the stronger surface winds and higher amount of sea spray may result in lower TC numbers.

Significant results are found for the observed dust AOD (AVHRR) in the NA starting at the 2.67% significance level, with an explained log-likelihood of 11% (figure not shown), but not for the modeled (GOCART) values. However, if we analyze the modeled dust AOD over the same time period as the observed AOD (i.e. 1982-2009), the pseudo-R^2 becomes 12% and is statistically significant. These results agree with the findings of Evan et al. (2006a) and Lau and Kim (2007), who identified an anti-correlation between NA tropical cyclone activity and observed dust cover. The GOCART model also shows a significant correlation or regression coefficient in the NI where dust mostly likely originates from the Great Indian Desert (Cinnam et al., 2006) or from west Asia (Dey et al., 2004).

3.2 Stratospheric variables associated with TC frequency

Here we analyze the role of lower stratospheric temperature on TC frequency, to address the open question of whether temperature variations in the stratosphere are related to TC activity. We also discuss the role of stratospheric aerosol loading (SAOD) in the EP and NA.

3.2.1 Lower stratospheric temperatures

We find that the lower stratospheric temperature is significantly associated with TC frequency only in the NA basin (Figure 3c). Both the temperature at 100 hPa and the SST/lower stratosphere temperature difference (i.e. SST – temperature at 100 hPa) show similar explained log-likelihoods of 27% and 31% respectively. The regression coefficient signs are negative for the temperature at 100 hPa and positive for the SST/lower stratosphere temperature difference in the NA. This may indicate that cooler temperatures at 100 hPa

favor TC development. Motivated by the finding in Vecchi et al. (2013) that changes in temperature in the upper troposphere at 300 hPa have a stronger influence on TC activity, we also analyzed changes in temperature at this level in all basins with significance only found in the NA, NI, and SI but none found in any of the basins for the SST/upper troposphere temperature difference (i.e. SST – temperature at 300 hPa, figure not shown). However, we would like to note that this problem is still unresolved as we did not use the method of decomposition as applied in Tang and Neelin (2004) where the principal component of NA SST and tropospheric temperature co-varied and explained most of their variance. It is further found that the temporal evolution of the SST/lower stratosphere temperature difference in the MERRA, ERA-Interim (figure not shown), and NCEP (figure not shown) reanalyses follow the variability of TC frequency very closely throughout the whole period in the NA (Figure 4a) but not in other basins. In agreement with this, Vecchi et al. (2013) recently suggested that lower stratospheric temperature trends may influence TC intensity in the tropical NA. In the EP and in all reanalyses (figure only shown for MERRA, Figure 4b), there are periods from around 1980 until 2000 where changes in the temperature at 100 hPa follow closely the variability of the TC frequency. However, we do not find significant pseudo-R^2 values for the lower stratospheric temperature in these basins except for the NA. Interestingly, while basins in the Northern Hemisphere display positive regression coefficients for the SST/lower stratosphere temperature difference (i.e. NA, EP, WP, NI), the others (i.e. SI, and SP) display negative ones, albeit not all statistically significant. For the temperature at 100 hPa, we see almost the opposite pattern with only clear negative regression coefficients in the WP (not significant) and NA associated with TC. This is further discussed in Section 4.4.

3.2.2 Stratospheric Aerosols

Except in the EP and NA, the SAOD generally does not show a high explained log-likelihood (Figures 3a and 3c, respectively). It is noteworthy that in the EP, SAOD gives the highest pseudo-R^2 value (25%). The SAOD's relation to TC frequency should be directly linked to aerosol radiative effects on the atmosphere and thermal structure. SAOD is strongly influenced by volcanic eruptions, which in turn generally warms the lower stratosphere and cools the surface (Evan, 2012). It is thus likely that the effect of changing SAOD on TC frequency is mediated by the lower stratospheric temperatures and SSTs, which would be in anti-phase with the TC frequency. However, SSTs show a significant positive regression coefficient in the EP, which would imply that cooling SSTs from a volcanic eruption lead to a decrease in the number of TCs. This is difficult to explain based on a simple analysis of direct aerosol radiative effects. More complex interactions, such as the potential link of SAOD and ENSO, which will be discussed in Section 4.1 may have to be invoked.

3.3 Circulation modes associated with TC frequency

Among the many modes of atmospheric circulation variability, the AMM and ENSO show the highest pseudo-R^2 values. The AMM and ENSO both display statistically significant pseudo-R^2 values of 27% in the NA and EP basins (Figures 3a and 3c), respectively. The pseudo-R^2 of ENSO is also significant in the NA (Figure 3c). Although the pseudo-R^2 for the AMM in the SI basin is only statistically significant at the 5% significance level, it is nonetheless worth mentioning. This shows that the AMM has strongly impacted the TC frequency in the NI and SI basins (figure not shown). The fact that the NAO shows no relation to the NA TC frequency will be discussed in Section 4. The role of the AMM in the NI and SI is opposite, with the former displaying a positive regression coefficient and the

latter a negative regression coefficient (figure not shown). This may be related to features of the large-scale circulation and will also be discussed in Section 4.2.

4. Discussion

4.1 Aerosols

The analysis presented in Section 3 supports several existing hypotheses on how different variables such as circulation indices, meteorological parameters and aerosol concentration/AOD are linked to TC frequency. A summary in terms of the change in the mean of the TC frequency for one unit of change in the variables, is presented in Figure 8. However, our results also indicate a number of non-trivial chains of events, in particular when it comes to aerosols. The patterns seen in the NA and the EP are particularly relevant in this respect. SAOD variability is strongly affected by volcanic eruptions, which lead to high aerosol concentrations in the stratosphere. An increased SAOD generally leads to a radiative surface cooling (lower SSTs), which would reduce the TC frequency in the EP and NA (Figure 3a and 3b). However, in the EP the higher SAOD values are associated with increased TC frequency. The reason could be that strong volcanic eruptions might favor El Niño-like conditions (e.g. Adams et al., 2003; Mann et al., 2005; Emile-Geay et al., 2008; Pausata et al., 2015a,b), leading to warmer SSTs over the EP. Specifically, Adams et al. (2003) found a 42% likelihood for such conditions to occur in the first year after a large eruption. Though the topic of whether a strong tropical volcanic eruption can trigger an El Niño is still controversial, our results are consistent with an SAOD-ENSO connection. To better understand the individual and combined impact of the radiative (SAOD-SST) and the SAOD-ENSO feedbacks on TCs frequency, ad-hoc sensitivity modelling studies need to be performed. As climate models improve in resolution and begin to resolve explicitly TC development, a better understanding of these relationships will be gained.

The BC and OC aerosol burdens were found to be strongly correlated with TC frequency in the NI Ocean basin. During the dry season (October to May), human-induced aerosol emissions cause a 3-km thick layer of pollution located over the NI Ocean and Indian sub-continent, commonly referred to as the atmospheric brown cloud (Ramanathan et al., 2005; Evan et al., 2011). This heats the lower troposphere through enhanced solar absorption, while cooling the surface due to solar reflection and absorption aloft (Meywerk and Ramanathan, 1999). Though our results do not conclusively demonstrate a causal link, they nonetheless indicate that anthropogenic aerosols in this basin are associated with increased TC activity. Whether this is due to direct radiative effects or to indirect effects mediated by changes in the large-scale circulation remains an open question. We further note that Wang et al. (2014) have reached a contrasting conclusion, namely that anthropogenic aerosols reduce TC activity. However, our results overall do not provide much observational/statistical support for Wang et al. (2014).

A number of studies, including this one, have found links between mineral dust and TCs in the NA (e.g. Evan et al., 2006a; Lau and Kim, 2007) and in the NI. In general, the outcome of aerosol interaction with TCs seems to be highly dependent on the basin and aerosol type, and indirect effects such as impacts on the large-scale circulation and modes of variability (*e.g.*, ENSO) can play a predominant role.

4.2 Large-scale modes of variability

The close link between circulation indices and a large number of other variables including aerosols often makes it challenging to determine a clear causal connection between the former and TC frequency. This complexity may be exemplified by the case of the AMO, which was found to have strong correlations with TC frequency across a range of basins, and in Mayfield (2005) is found to act as the main driver of NA hurricane activity. The importance of the AMO in modulating TC frequency has been discussed by Goldenberg et al. (2001) and Zhang and Delworth (2006), while Vimont and Kossin (2007) identified an in-phase relationship between the AMO and AMM and hurricane activity in the NA. A positive AMO or AMM causes a northward shift of the ITCZ. This weakens the surface easterly winds and the upper level westerlies over the NA, causing a reduction in the vertical wind shear and a resulting increase in TC activity. The present study also finds an in-phase relationship in the NI Ocean and an out-of-phase one in the SI Ocean (figure not shown). However, we do not find a link between the wind shear and TC frequency in these basins, suggesting that other changes in large-scale circulation may dominate the modulation of TC activity. This may also imply that the diabatic heating that is induced by a positive AMO, which is a proxy for the vertical wind shear (Hannachi and Turner, 2013), is not strong enough to influence TC activity. The fact that, in the SI, the latter is out-of-phase with TC frequency could be explained by the fact that the atmospheric flow is opposite to that in the NI (e.g., Goswami et al., 2003).

Another result from the analysis of the modes of variability which requires some discussion is the apparent lack of influence of the NAO on the NA. Intuitively, the NAO might be expected to have a strong effect on any atmospheric phenomenon developing in the NA basin. In fact, there is a known link between the frequency of intense cyclones in the North Atlantic and windstorms in the Euro-Atlantic sector and the NAO (*e.g.* Pinto et al., 2009; Messori and Caballero, 2015), suggesting that our data for the frequency of cyclones of all intensities should show a significant pseudo-R^2 value. However, this influence is typically seen in the extra-tropical domain, and generally pertains to mid-latitude storms. Moreover, the NAO explains less variance during a large part of the tropical cyclone season than during the winter months, and previous analyses have suggested that a direct NAO-TC link is not as obvious as might be intuitively expected (Mestre and Hallegatte, 2009).

4.3 East Pacific and North Atlantic inverse relationship

One striking result is the opposite relationship found in the sign of the regression coefficients of all the circulation indices (i.e. ENSO, NAO, QBO, and AMM) for the EP and NA (Figure 3). The same holds for most of the meteorological and aerosol variables except: SSTs, BC and SS AOD, and precipitable water. This result is in agreement with Wang and Lee (2009) and Collins (2010), which shows the robustness of our results and methodology. A proposed explanation is that ENSO is the underlying reason for the opposite relationship (Tang and Neelin, 2004; Collins, 2007; 2010). During El Niño events, the EP displays warmer SSTs due to weakened trade winds and enhanced RH in the boundary layer, which can cause an increase in TC activity (Collins, 2010). This hypothesis is in agreement with our results, which show a positive regression coefficient between ENSO and TC frequency in the EP basin (Figure 3a). In the NA (Figure 3c), the lower level RH (1000-850 hPa), ENSO and the wind shear all act to suppress TCs – a result that is well-established in the literature (e.g.

Gray and Sheaffer. 1991; Camargo et al., 2007; Collins, 2010). The low-level RH explains 14% of the log-likelihood in the basin, and the NA is the only basin where the wind shear's link to TC frequency is statistically significant (pseudo-R^2 of 28%). The relationship with wind shear in the EP, as well as in the other basins, is not so clear. Collins (2007; 2010) found the same result for the EP, but offered no explanation.

4.4 Lower Stratospheric Temperatures

The recent literature on the influence of lower stratospheric temperatures on TCs has largely focused on the potential intensity of the cyclones, as opposed to their frequency. However, the assertion that lower stratospheric temperature might also affect TC frequency is not entirely destitute of basis. Wang et al. (2014) pointed out that tropopause temperatures have a larger natural variability on seasonal, interannual and decadal time scales than the SSTs, and that upper-atmospheric temperature influences TC intensity. Our results suggest that, at least in some basins, atmospheric temperature at 100 hPa (T100) is correlated with TC frequency (Figure 3). Our analysis further reveals a possible dipole relationship between the basins in the Northern and Southern Hemispheres that should be tested by model simulations. This pattern links back to the role of aerosols and volcanic eruptions discussed above. There is a clear increase in lower stratospheric temperatures in all basins matching the 1982 El Chichón and 1991 Mount Pinatubo volcanic eruptions (for further details, see Vecchi et al., 2013). In the EP, the running mean curves of the temperature at 100 hPa and TC frequency during the years of the eruptions show a striking correspondence (Figure 5a). The opposite occurs in the NA, with a clear reduction in TC frequency in the years immediately following the eruptions (Figure 5b). While it is difficult to determine whether these are more than mere coincidences, the Poisson regression method suggests a high level of statistical significance in the NA.

In general, it remains difficult to assess the impact of lower stratospheric temperatures on TC activity due to observational issues related to discrepancies in upper tropospheric temperature in the reanalysis datasets (Vecchi et al., 2013). Even though climate models are able to reproduce TC interannual variability and activity (Zhao et al., 2009; Chen and Lin, 2013; Wu et al., 2014), some climate models do not properly simulate recent cooling trends in the lower stratosphere, due to a lack of key processes involving volcanic eruptions and ozone depletion (Emanuel et al., 2013). In order to obtain robust projections of future TC activity, it therefore seems necessary to address the ability of climate models to properly simulate lower stratospheric temperatures, at least in the EP and NA. Motivated by this consideration, we test whether a CMIP5 multi-model mean (MMM) for the period 1950-2005 was successful in simulating the general lower stratospheric cooling due to enhanced concentrations of greenhouse gases. Figure 6 shows the time-latitude 100 hPa temperature from the MMM (Figure 6a) versus the MERRA, ERA-Interim, and NCEP/NCAR reanalyses (Figure 6b-d, respectively). The MMM clearly shows the signature of the Mount Agung eruption in 1963 with a temperature anomaly between 0.3 and 0.7 °C. This is followed by a slight cooling over the period 1965-1982, with a maximum of about -0.5 °C centered around the tropics**.** A rapid warming then took place after the El Chichón eruption in 1982, with a maximum temperature anomaly of about 0.7 °C, peaking near 30° N. However, this maximum warming is weaker by about 0.5 °C compared to MERRA and ERA-Interim and by about 0.8 °C compared to NCEP. Unlike the MMM and NCEP, MERRA and ERA-Interim also show a maximum centered around the North and South mid-latitudes. Discrepancies are also found for the Mount Pinatubo eruption in 1991. Following the Pinatubo warming, the NCEP datasets shows a strong, persistent global cooling, while MERRA and ERA-Interim show weaker, briefer signals. The cooling in the MMM is limited to the mid-latitudes, and peaks roughly four years before the cooling shown in the reanalyses.

Next, we analyze the vertical distribution of the temperature trends over different periods for MERRA, ERA-Interim, and NCEP/NCAR (Figure 7a-c) as well as the MMM (Figure 7d). The cooling at 100 hPa is at least twice as large in the NCEP/NCAR reanalysis than in the MMM, MERRA, and ERA-Interim, whereas the vertical profiles at lower altitudes display reasonably consistent patterns. It is interesting to note that the 30 hPa level also shows pronounced anomalies in MERRA, ERA-Interim, and MMM, especially during the period 1990-1999 (Figures 7e, 7f, and 7h, respectively). Previous studies, however, suggest that temperature changes at this level (30 hPa) do not significantly influence TC intensity (Vecchi et al., 2013). Vecchi et al. (2013) and Emanuel et al. (2013) also noted that lower stratospheric temperatures in the NCEP/NCAR data are cooler than those of other reanalysis datasets. Therefore, while the CMIP5 models may struggle to properly reproduce lower stratospheric temperature changes, there is no agreement between the different reanalyses either.

5. Summary and conclusions

The statistical relationship between seasonal mean environmental variables and tropical cyclone (TC) frequency was investigated for the period 1980-2009 in six TC development regions (Eastern, Western and Southern Pacific, Northern and Southern Indian and North Atlantic Oceans). A generalized linear model based on the Poisson regression was used to determine statistically significant links between meteorological variables, aerosols, and large-scale modes of variability and TC frequency in the different basins. The main findings are summarized below:

1) ENSO is found to be significantly associated with TC frequency in the Eastern Pacific and negatively associated with TC frequency in the North Atlantic. TC frequency was also found to be significantly negatively associated with RH (1000-

850hPa) and vertical wind shear (u 200 – u 850 hPa) over the North Atlantic. These results are in line with previous studies, such as Wang and Lee (2009) and Collins (2010), and support the idea that ENSO is both directly linked to TC activity in these two basin and also acts to amplify the effect of a number of variables on TC frequency (*e.g.* Tang and Neelin, 2004; Camargo et al., 2007).

2) The explained log-likelihoods of AMM and ENSO are 24-27% in the East Pacific, North Atlantic, and North Indian. These results are in line with previous studies (*e.g.*, Collins, 2007, 2010; Trenberth and Shea, 2006; Vimont and Kossin, 2007). We further find an inverse relationship in the North Indian and South Indian, but the result for SI is not significant. Due to a low explained log-likelihood for wind shear in these two development regions, we suggest that changes in large-scale circulation plays a dominant role in the modulations of TC frequency.
3) The relationship between SSTs and TC frequency is not as strong as that found for some of the other variables. Nonetheless, there are still significant explained log-likelihoods in the Eastern Pacific, North Atlantic, South Indian and South Pacific, whereas no significance was found in the Western Pacific and North Indian basins, in agreement with Chan and Liu (2004) and Ng and Chan (2012). The explained log-likelihood of the relative SSTs is nearly double that of the absolute SSTs in the North Atlantic and South Pacific. This is in line with the findings in Vecchi and Soden (2007, 2008), Swanson (2008), and Camargo et al. (2013) where relative SST anomalies play a larger role in affecting TC potential intensity than absolute SST anomalies. Wind shear is only significantly correlated in the North Atlantic, as already noted by Aiyyer and Thorncroft (2011).
4) Tropospheric black carbon and organic carbon aerosols are found to be significantly related to TC frequency in the North Indian Ocean. These aerosols can cause

tropospheric warming and surface cooling (Meywerk and Ramanathan, 1999), which ultimately may modify the monsoon circulation, reduce the vertical wind shear and increase TC activity (Evan et al., 2011). We also found a positive relationship between sea salt and organic aerosols and TC frequency in the South Pacific, which could be related to an increase in surface heat exchange between the ocean's surface and atmosphere leading to a larger latent and sensible heating.

5) A link is found between observed dust aerosol optical depth and TC frequency in the North Atlantic while the role of modeled dust AOD is only significant in the North Indian basin. The modeled dust AOD only becomes significant in the North Atlantic during a limited time period. These results are in line with Evan et al. (2006a) and Lau and Kim (2007), at least in the North Atlantic.
6) Stratospheric aerosol optical depth was found to be the variable with the highest explained log-likelihood in the Eastern Pacific. We hypothesize that the effect of stratospheric aerosols on TC frequency occurs both through direct effects on radiation, causing stratospheric warming and surface cooling (Evan, 2012), and by an indirect process mediated by circulation changes favoring El Niño-like conditions (Adams et al., 2003).
7) The effect of the lower stratospheric temperature on TC frequency was strongest in the North Atlantic with an explained log-likelihood of 28% and with a negative regression coefficient. This result indicates that cooler temperatures at this level increase TC frequency, and complements results in the literature relative to their role in enhancing cyclone potential intensity (*e.g.* Vecchi et al., 2013; Emanuel et al., 2013).
8) A stratospheric warming following the eruptions of El Chichón and Mount Pinatubo is found in all the reanalyses (i.e. MERRA, ERA-Interim, and NCEP/NCAR) as

well as in the multi-model mean from five CMIP5 models. However, the temperature anomalies in the multi-model mean were smaller by approximately 0.5-0.8 °C compared to the reanalyses. Though it is difficult at the present time to assess the accuracy of the reanalyses, the large model bias may affect projections of the future intensity and frequency of TCs.

The relevant variables identified in the analysis can be linked to dynamical and radiative forcing processes that influence TC development and hence frequency. The potential effect of aerosols and lower stratospheric temperatures on TC activity has not been well documented previously. The present paper also uncovers novel relationships, such as that between the AMM and the TC frequency in the North and South Indian Oceans. The broad range of connections between variables and TC frequency tested here constitutes a first step in building a global observations- based framework for understanding and monitoring TC development and evaluating the ability of models to accurately simulate TCs. We envisage adopting a multivariate multiple regression approach in a future study and looking at time-lagged relationships between the variables and TC frequency, as well as using principal component analysis to analyze more thoroughly the correlations between variables. Future studies will benefit from the integrated global observing systems developed by the World Meteorological Organization (WMO) and other international observational science organizations. Such efforts should in particular focus on stratospheric processes, which have been shown to affect TC development.

Appendix

The results of the Poisson regression applied to the NCEP, ERA-Interim, and MERRA reanalyses (Figure 9) show a good agreement for SSTs and relative SSTs in all basins, and for all significant variables in the NA. The differences between the explained log-likelihoods of SSTs and relative SSTs among all the datasets differ by less than 5%. In the NA, the discrepancies are modest for most variables: 15% for the SST/lower stratosphere temperature difference (SST-T100 hPa), 16% for the temperature at 100 hPa, and of less than 5% and 6% for the windshear and precipitable water, respectively. Always in the NA, ERA-Interim shows the lowest pseudo-R^2 values for the SSTs and relative SSTs, and the largest values for the temperature gradient, temperature at 100 hPa and windshear. From these results we conclude that, although there are important differences between the datasets, it is nonetheless possible to draw some robust conclusions on the influence of individual variables on TC frequency by applying the statistical technique of Poisson regression.

Acknowledgments

This study was financially supported by the Bolin Centre for Climate Research, the Department of Meteorology at the University of Stockholm, and the Swedish Vetenskapsrådet (MILEX project). The IBTrACS dataset was obtained from the NOAA National Climatic Data Center (https://www.ncdc.noaa.gov/ibtracs/). NCEP reanalysis data was retrieved from the NOAA Earth Systems Research Laboratory (http://www.esrl.noaa.gov/psd/data/gridded/data.ncep.reanalysis.html). ERA-Interim data was taken from the European Centre for Medium-Range Weather Forecasts (http://apps.ecmwf.int/datasets/). MERRA data was obtained from the Modeling and the Assimilation Data and Information Services Center (MDISC) at NASA Goddard (http://disc.sci.gsfc.nasa.gov/daac-bin/DataHoldings.pl). All circulation indices were obtained from the NOAA Earth Systems Research Laboratory (http://www.esrl.noaa.gov/psd/data/climateindices/list/). Observed dust AOD was obtained from the Atlantic Aerosol Products on http://evan.ucsd.edu/Data.html.

References

Adams, J. B., M. E. Mann, and C.M. Ammann (2003), Proxy evidence for an El Nino-like Response to Volcanic Forcing. *Nature*, 426, 274-278.

Aiyyer, A., C. Thorncroft (2011), Interannual-to-multidecadal variability of vertical shear and tropical cyclone activity, J. Clim., 24, 2949-2962.

Ambaum, M. H. P., B. J. Hoskins, and D. B. Stevenson (2001), Arctic Oscillation or North Atlantic Oscillatiion?, J. Clim. 14, 3495-35077.

Barnston A. G,. R. E. Livezey (1987), Classification, seasonality and persistence of low-frequency atmospheric circulation patterns, Monthly Weather Review, 115, 1083–1126.

Basher, R., and X. Zheng (1995), Tropical cyclones in the southwest Pacific: Spatial patterns and relationships to the Southern Oscillation and sea surface temperature, J. Clim., 8, 1249-1260.

Bengstsson, L., K. I. Hodges, M. Esch, N. Keenlyside, L. Kornblueh, J.-J. Luo, T. Yamagata (2007), How may tropical cyclones change in a warmer climate?, Tellus A, 59, 539-561, DOI: 10.1111/j.1600-0870.2007.00251.x.

Bond, T.C. et al. (2007), Historical emissions of black and organic carbon aerosol from energy-related combustion, 1850-2000. Global Biogeochem. Cycles, 21, GB2018, doi: 10.1029/2006GB002840.

Booth, B. B. B., N. J. Dunstone, P. R. Halloran, T. Andrews, and N. Bellouin (2012), Aerosols implicated as a prime driver of twentieth-century North Atlantic climate variability, Nature, 484, 228-232, doi:10.1038/nature10946.

Camargo, S. J.; K. A. Emanuel, and A. H. Sobel (2007), Use of a genesis potential index to diagnose ENSO effects on tropical cyclone genesis, Journal of Climate, 20, 4819-4834.

Camargo, S. J. (2013), Global and regional aspects of tropical cyclone activity in the CMIP5 models, J. Clim., 26, 9880-9902, doi: 10.1175/JCLI-D-12-00549.1.

Camargo, S. J., M. Ting, and Y. Kushnir (2013), Influence of local and remote SST on North Atlantic tropical cyclone potential intensity, Climate Dyn.,40,1515–1529, doi:10.1007/s00382-012-1536-4.

Cameron, A. C., and F. A. G. Windmeijer (1996), R-Squared measures for Count Data Regression Models with Applications to Health Care Utilization, Journal of Business and Economic Statistics, 14, 209-220.

Caron, L.-P., M. Boudreault, C. L. Bruyere (2014), Changes in large-scale controls of Atlantic tropical cyclone activity with the phases of the Atlantic multidecadal oscillation, Clim. Dyn., 44, 1801–182, DOI 10.1007/s00382-014-2186-5.

Chan, J. C. L. (1995), Tropical cyclone activity in the western North Pacific in relation to the stratospheric quasi-biennial oscillation., Mon. Wea. Rev., 123, 2567-2571.

Chan J. C. L., K. S. Liu (2004), Global warming and western North Pacific typhoon activity from an observational perspective, J. Climate, 17, 4590–4602.

Chen, J.-H., and S.-J. Lin (2013), Seasonal Predictions of Tropical Cyclones Using a 25-km-Resolution General Circulation Model, J. Clim., 26, 380-398, doi: http://dx.doi.org/10.1175/JCLI-D-12-00061.

Chiang, J. C. H., and D. J. Vimont (2004), Analagous meridional modes of atmosphere-ocean variability in the tropical Pacific and tropical Atlantic, J. Climate, 17(21), 4143-4158.

Chinnam, N., S. Dey, S. N. Tripathi, and M. Sharma (2006), Dust events in Kanpur (northern India): chemical evidences for source and implications to radiative forcing, Geophys. Res. Lett., 33, L08803. http://dx.doi.org/10.1029/2005GL025278.

Chin, M., P. Ginoux, S. Kinne, O. Torres, B. N. Holben, B. N. Duncan, R. V. Martin, J. A. Logan, A. Higurashi, and T. Nakajima (2002), Tropospheric aerosol optical thickness from the GOCART model and comparisons with satellite and sunphotometer measurements, J. Atmos. Sci., 59, 461-483.

Chin, M., T. Diehl, Q. Tan, J. M. Prospero, R. A. Kahn, L. A. Remer, H. Yu, A. M. Sayer, H. Bian, I. V. Geogdzhayev, B. N. Holben, S. G. Howell, B. J. Huebert, N. C. Hsu, D. Kim, T. L. Kucsera, R. C. Levy, M. I. Mishchenko, X. Pan, P. K. Quinn, G. L. Schuster, D. G. Streets, S. A. Strode, O. Torres, and X.-P. Zhao (2014), Multi-decadal variations of atmospheric aerosols from 1980 to 2009: Sources and regional trends, Atmos. Chem. Phys., 14, 3657-3690, doi:10.5194/acp-14-3657-2014.

Chung, C. E., V. Ramanathan (2006), Weakening of North Indian SST gradients and the monsoon rainfall in India and the Sahel, J. Climate, 19, 2036–2045.

Chylek, P., and G. Lesins (2008), Multidecadal variability of Atlantic hurricane activity: 1851–2007, J. Geophys. Res., 113, doi: 10.1029/2008JD010036.

Collins, J. M. (2007), The relationship of ENSO and relative humidity to interannual variations of hurricane frequency in the North-East Pacific ocean, Papers of the Applied Geography Conferences, 30:324–333.

Collins, J. M. (2010), Contrasting High North-East Pacific Tropical Cyclone Activity with Low North Atlantic Activity, Southeastern Geographer, Volume 50, Number 1, pp. 83-98. Published by The University of North Carolina Press, DOI: 10.1353/sgo.0.0069.

Dee, D. P., S. M. Uppala, A. J. Simmons, P. Berrisford, P. Poli, S. Kobayashi, U. Andrae, M. A. Balmaseda, G. Balsamo, P. Bauer, P. Bechtold, A. C. M. Beljaars, L. van de Berg, J. Bid-lot, N. Bormann, C. Delsol, R. Dragani, M. Fuentes, A. J. Geer, L. Haimberger, S. B. Healy, H. Hersbach, E. V. Holm, L. Isaksen, P. Kallberg, M. Kohler, M. Matricardi, A. P. McNally, B. M. Monge-Sanz, J. J. Morcrette, B. K. Park, C. Peubey, P. de Rosnay, C. Tavolato, J. N. Thepaut, and F. Vitart (2011), The ERA-Interim reanalysis: configuration and performance of the data assimilation system, Quart. J. R. Meteorol. Soc., 137, 553-597, DOI: 10.1002/qj.828.

Dey, S., S. N. Tripathi, R. P. Singh, B. N. Holben (2004), Influence of dust storms on the aerosol optical properties over the Indo–Gangetic Basin, J. Geophys.Res. 109 (D20), 1–13, http://dx.doi.org/10.1029/2004JD004924.

Diro, G. T., F. Giorgi, R. Fuentes-Franco, K. J. E. Walsh, G. Guliani, and E. Coppola (2014), Tropical cyclones in a regional climate change projection with RegCM4 over the CORDEX Central America domain, Climate Change, 125:79-94, DOI 10.1007/s10584-014-1155-7.

Dong, K., and G. J. Holland (1994), A global view of the relationship between ENSO and tropical cyclone frequencies, Acta Meteor. Sinica, 8, 19-29.

Dunstone, N. J., D. M. Smith, B B. B. Booth, L. Hermanson, and R. Eade (2013), Anthropogenic aerosol forcing of Atlantic tropical storms, Nature Geoscience, 6, 534–539, doi:10.1038/ngeo1854.

Elsner J.B, Bossak B.H, Niu X.-F (2001), Secular changes to the ENSO–U.S. hurricane relationship, Geophys. Res. Lett. 28, 4123–4126. doi:10.1029/2001GL013669.

Emanuel, K. A. (1987), The dependence of hurricane intensity on climate, Nature, 326, 483-485.

Emanuel, K.A. (2013), Downscaling CMIP5 climate models shows increased tropical cyclone activity over the 21st century, Proc. Nat. Acad. Sci., 110, doi/10.1073/pnas.1301293110.

Emanuel, K. A., and D. S. Nolan (2004), Tropical cyclone activity and global climate, Bull. Amer. Metror. Soc., 85 (5), 666–667.

Emanuel, K., A., and A. Sobel (2013), Response of tropical sea surface temperature, precipitation, and tropical cyclone-related variables to changes in global and local forcing, J. Adv. Model. Earth Sys.,5,447–458, doi:10.1002/jame.20032.

Emanuel, K., S. Solomon, D. Folini, S. Davis, and C. Cagnazzo (2013), Influence of Tropical Tropopause Layer Cooling on Atlantic Hurricane Activity, J. Climate, 26, 2288–2301.

Emile-Geay, J., R. Seager, M. A. Cane, E. R. Cook, and G. H. Haug (2008), Volcanoes and ENSO over the Past Millennium, J. Clim. 21, 3134–3148.

Evan, A. T., J. Dunion, J. A. Foley, A. K. Heidinger, and C. S. Velden (2006a), New evidence for a relationship between Atlantic tropical cyclone activity and African dust outbreaks, Geophys. Res. Lett., 33, L19813, doi:10.1029/2006GL026408.

Evan, A. T., S. Mukhopadhyay (2010), African Dust over the Northern Tropical Atlantic: 1955–2008, J. Appl. Met. & Clim., 49, 2213-2229, doi: 10.1175/2010JAMC2485.1.

Evans, J. I., and R. J. Allan (1992), El Nino/Southern Oscillation modification to the structure of the monsoon and tropical cyclone activity in the Australian region, Int. J. Climatol., 12, 611-623.

Evan, A. T., J. P. Kossin, C. E. Chung, and V. Ramanathan (2011), Arabian Sea tropical cyclones intensified by emissions of black carbon and other aerosols, Nature, 479, 94–97, doi:10.1038/nature10552.

Evan, A. T. (2012), Atlantic hurricane activity following two major volcanic eruptions, J. Geophys. Res., 117, doi:10.1029/2011JD016716.

Evans, J. L., and R. J. Allan (1992), El Niño/Southern Oscillation modification to the structure of the monsoon and tropical cyclone activity in the Australian region, Int. J. Climat., 12, 611-623.

Fairall, C. W., J. D. Kepert, and G. H. Holland (1994), The effect of sea spray on surface energy transports over the ocean, Global Atmos. Ocean Syst., 2, 121–142.

Frank, W. M., and G. S. Young (2007), The interannual variability of tropical cyclones, Mon. Weath. Rev., 135, 3587–3598.

Goldenberg, S.B., and L. J. Shapiro (1996), Physical Mechanisms for the Association of El Niño and West African Rainfall with Atlantic Major Hurricane Activity, J. Climate, 9, (6):1169-1187,

Goldenberg, S. B., C. W. Landsea, A. M. Mestas-Nuñez, and W. M. Gray (2001), The recent increase in Atlantic hurricane activity: Causes and implications, Science, 293, 474–479.

Goswami, B. N., R. S. Ajayamohan, P. K. Xavier, and D. Sengupta (2003), Clustering of synoptic activity by Indian summer monsoon intraseasonal oscillations, Geophys. Res. Lett., 30, doi: 10.1029/2002GL016734.

Gray, W. M. (1984a), Atlantic seasonal hurricane frequency: Part 1. El Niño and 30 mb quasi-biennial oscillation influences, Mon. Wea. Rev., 112, 1649-1668.

Gray, W. M. (1984b), Atlantic seasonal hurricane frequency, Part II: forecasting its variability. Mon. Wea. Rev., 112, 1669-1683.

Gray, W. M., and J. D. Sheaffer (1991), El Niño and QBO influences on tropical cyclone activity, In Teleconnections linking worldwide climate anomalies, edited by M. H. Glantz, R. W. Katz, and N. Nicholls, 257–84. New York: Cambridge University Press.

Hannachi, A., S. Unkel, N. T. Trendafilov, and I. T. Jolliffe (2009), Independent component analysis of climate data: A new look at EOF rotation, J. Climate, 22, 2797-2812.

Hannachi, A., and A. G. Turner (2013), 20th century intraseasonal Asian monsoon dynamics viewed from Isomap, Nonlin. Processes Geophys., 20, 725-741, doi: 10.5194/npg-20-725-2013.

Heinzl, H., and M. Mittlbock (2003), Pseudo R-squared measures for Poisson regression models with over- or underdispersion, Computational Statistics & Data Analysis, 44, 253 – 271.

Holland G. J (1997), The maximum potential intensity of tropical cyclones, J. Atmos. Sci., 54, 2519–2541, doi:10.1175/1520-0469(1997)054<2519:TMPIOT>2.0.CO;2.

IPCC (2013), Climate Change 2013: The Physical Science Basis. Contribution of Working Group I to the Fifth Assessment Report of the Intergovernmental Panel on Climate Change, Chapter 7 [Stocker, T.F., D. Qin, G.-K. Plattner, M. Tignor, S.K. Allen, J. Boschung, A. Nauels, Y. Xia, V. Bex and P.M. Midgley (eds.)], Cambridge University Press, Cambridge, United Kingdom and New York, NY, USA, 1535 pp, doi:10.1017/CBO9781107415324.

Kalnay, E., M. Kanamitsu, R. Kistler, W. Collins, D. Deaven, L. Gandin, M. Iredell, S. Saha, G. White, J. Woollen, Y., Zhu, A. Leetmaa, B. Reynolds, M. Chelliah, W. Ebisuzaki, W. Higgins, J. Janowiak, K. Mo, C. Ropelewski, J. Wang, R. Jenne, and D. Joseph (1996), The NCEP/NCAR 40-Year Reanalysis Project, Bull. Amer. Meteor. Soc., 77, 437–471.

Kaplan, A., Y. Kushnir, M. A. Cane, and M. B. Blumenthal (1997), Reduced space optimal analysis for historical data sets: 136 years of Atlantic sea surface temperatures, J. Geophys. Res., 102, 27,835-27,860.

Klotzbach, P. J. (2006), Trends in global tropical cyclone activity over the past twenty years, Geophys. Res. Lett., 33, doi:10.1029/2006GL025881.

Klotzbach, P. J., and W. M. Gray (2008), Multidecadal Variability in North Atlantic Tropical Cyclone Activity, J. Climate, 21, 3929–3935, doi: http://dx.doi.org/10.1175/2008JCLI2162.1.

Knapp, K. R., M. C. Kruk, D. H. Levinson, H. J. Diamond, and C. J. Neumann (2010), The International Best Track Archive for Climate Stewardship (IBTrACS), Bulletin of the American Meteorological Society, 91, 363-376, 2010.

Knutson, R. Thomas, J. L. McBride, J. Chan, K. Emanue, G. Holland, C. Landsea, I. Held, J. P. Kossin, A. K. Srivastava, S. Masato (2010), Tropical Cyclones and Climate. Change, Nature Geosci., 3.3, 157-163, doi:10.1038/ngeo779.

Kuleshov, Y., and G. de Hoedt (2003), Tropical cyclone activity in the Southern Hemisphere, Bull. Aust. Meteorol. Oceanogr. Soc., 16, 135 – 137.

Kopke, P. Hess, H. Schult, and E. Shettle, E. (1997), The Global Aerosol Data Set (GADS), MPI-Rep., Hamburg 243, 44.

Kossin, J. P., K. R. Knapp, D. J. Vimont, R. J. Murnane, and B. A. Harper (2007), A globally consistent reanalysis of hurricane variability and trends, Geophys. Res. Lett., 34, L04815, doi:10.1029/2006GL028836.

Kossin, J. P., T. L. Olander, and K. R. Knapp (2013), Trend Analysis with a new global record of tropical cyclone intensity, J. Clim., 26, 9960-9976, DOI: 10.1175/JCLI-D-13-00262.1.

Kruk, M. C., K. R. Knapp, and D. H. Levinson (2010), A technique for merging global tropical cyclone best track data, J. Atmos. Oceanic Tech., 27,680-692, doi:10.1175/2009JTECHA1267.1

Kunkel, K. E., et al. (2013), Monitoring and understanding trends in extreme storms, Bul. Amer. Meteor. Soc., 94, 499-514.

Landsea, C. W., and W. M. Gray (1989), Eastern North Pacific tropical cyclone climatology--low frequency variations, Report of WG, WMO, WMO/TD, no. 319, Geneva, 1989.

Landsea, C. W., R. A., Jr., Pielke, A. M. Mestas-Nuñez, J. A. Knaff (1999), Atlantic basin hurricanes: Indices of climatic changes, Climatic Change, 42, 89-129.

Landsea, C. W., C. Anderson, N. Charles, G. Clark, J. Dunion, J. Fernandez-Partagas, P. Hungerford, C. Neumann, and M. Zimmer (2004), The Atlantic hurricane database re-analysis project: Documentation for the 1851–1910 alterations and additions to the HURDAT database, in Hurricanes and Typhoons: Past, Present and Future, edited by R. J. Murname and K.-B. Liu, pp. 177– 221, Columbia Univ. Press, New York.

Landsea, C. W., B. A. Harper, K. Hoarau, J. A. Knaff (2006), Can we detect trends in extreme tropical cyclones?, Science, 313, 452-454.

Latif, M., N. S. Keenlyside, and J. Bader (2007), Tropical sea surface temperature, vertical wind shear, and hurricane development, Geophys. Res. Lett., 34, L01710.

Lau, K. M., and K. M. Kim (2007), Cooling of the Atlantic by Saharan dust, Geophys. Res. Lett., 34, L23811, doi:10.1029/2007/GL031538.

Messori, G. and R. Caballero (2015), On double Rossby wave breaking in the North Atlantic, J. Geophys. Res. Atm., 120, 21, 11,129-11,150, 10.1002/2015JD023854.

Mann, M. E., M. A. Cane, S. E. Zebiak, and A. Clement (2005), Volcanic and Solar Forcing of the Tropical Pacific over the Past 1000 Years, J. Clim. 18, 447–456.

Mann, M. E., and K. A. Emanuel (2006), Atlantic hurricane trends linked to climate change, EOS, 87, 233-244.

Mantua, N. J., S. R. Hare, Y. Zhang, J. M. Wallace, and R.C. Francis (1997), A Pacific decadal climate oscillation with impacts on salmon, Bulletin of the American Meteorological Society, 78, 1069-1079.

Mayfield, M. (2005), Testimony for oversight hearing before Committee on Commerce, Science and Transportation, Subcommittee on Disaster Prevention and Prediction, U.S. Senate, on ‘‘The Lifesaving Role of Accurate Hurricane Prediction,’’ Washington, D. C.

Meehl, G., J. Arblaster, J., W. Collins (2008), Effects of black carbon aerosols on the Indian monsoon, J. Clim. 21, 2869–2882.

Mestre, O., and S. Hallegatte (2009), Predictors of Tropical Cyclone Numbers and Extreme Hurricane Intensities over the North Atlantic Using Generalized Additive and Linear Models, J. Climate, 22, 633–648, doi: http://dx.doi.org/10.1175/2008JCLI2318.1.

Meywerk, J, Ramanathan V. (1999), Observations of the spectral clear-sky aerosol forcing over the tropical Indian Ocean, J. Geophys. Res., 104, 24359-24370.

Murakami, H., et al. (2012a), Future changes in tropical cyclone activity projected by the new high-resolution MRI-AGCM, J. Clim.,25,3237– 3260.

Murakami, H. (2014), Tropical cyclones in reanalyses datasets, Geophys. Res. Lett., 41, 2133-2141, doi:10.1002/2014GL059519.

Ng, E. K. W., and J. C. L. Chan (2012), Interannual variations of tropical cyclone activity over the north Indian Ocean, Int. J. Climatol., 32: 819–830, DOI: 10.1002/joc.2304.

Nicholls, N. (1979), A possible method for predicting seasonal tropical cyclone activbity in the Australian region, Mon. Wea. Rev., 107, 1221-1224.

Nicholls, N. (1984), The southern oscillation, sea-surface-temperature, and interannual fluctuations in Australian tropical cyclone activity, J. Climate. 4, 661-670.

Nicholls, N., C. Landsea, J. Gill (1997a), Recent Trends in Australian Region Tropical Cyclone Activity, Meteorol. Atmos. Phys., 65, 197-205.

Oouchi, K., J. Yoshimura, H. Yoshimura, R. Mizuta, S. Kusunoki, and A. Noda (2006), Tropical cyclone climatology in a global-warming climate as simulated in a 20km-mesh global atmospheric model: Frequency and wind intensity analysis, J. Meteorol. Soc. Jpn., 84, 259– 276.

Pausata, F. S. R., L. Chafik, R. Caballero, D. S. Battisti (2015a), Impacts of high-latitude volcanic eruptions on ENSO and AMOC, PNAS, 13784–13788, doi: 10.1073/pnas.1509153112.

Pausata, F. S. R., A. L. F. Grini , R. Caballero, A. Hannachi , and Ø. Seland (2015b), High-latitude volcanic eruptions in the Norwegian Earth System Model: the effect of different initial conditions and of the ensemble size, Tellus B, 67, 26728, http://dx.doi.org/10.3402/tellusb.v67.26728.

Pinto, J.G., S. Zacharias, A. H. Fink, G. C. Leckebusch, and U. Ulbrich (2009), Factors contributing to the development of extreme North Atlantic cyclones and their relationship with the NAO, Clim. Dyn., 32, 711-737.

Ramanathan, V., C. Chung, D. Kim, T. Bettge, L. Buja, J. T. Kiehl, W. M. Washington, Q. Fu, D. R. Sikka, and M. Wild (2005), Atmospheric brown clouds: Impacts on South Asian climate and hydrological cycle, Proceedings of the National Academy of Sciences of the USA, 10.1073/pnas.0500656102.

Ramsay, H. A. (2013), The Effects of Imposed Stratospheric Cooling on the Maximum Intensity of Tropical Cyclones in Axisymmetric Radiative–Convective Equilibrium, J. Climate, 26, 9977–9985.

Revell, C., and S. Goulter (1986), South Pacific tropical cyclones and the Southern Oscillation, Mon. Wea. Rev., 114**,** 1138–1144.

Rienecker, M. M., M. J. Suarez, R. Gelaro, R. Todling, J. Bacmeister, E. Liu, M. G. Bosilovich, S. D. Schubert, L. Takacs, G.-K. Kim, S. Bloom, J. Chen, D. Collins, A. Conaty, A. da Silva, et al. (2011), MERRA: NASA's Modern-Era Retrospective Analysis for Research and Applications, J. Climate, 24, 3624-3648, doi:10.1175/JCLI-D-11-00015.1.

Sabbatelli, T. A., and M. E. Mann (2007), The influence of climate state variables on Atlantic Tropical Cyclone occurrence rates, J. Geophys. Res., 112, D17114, doi:10.1029/2007JD008385.

Santer, B. D., T. M. L. Wigley, P. J. Gleckler, C. Bonfils, M. F. Wehner, K. AchutaRao, T. P. Barnett, J. S. Boyle, W. Brüggemann, M. Fiorino, N. Gillett, J. E. Hansen, P. D. Jones, S. A. Klein, G. A. Meehl, S. C. B. Raper, R. W. Reynolds, K. E. Taylor, and W. M. Washington (2006), Forced and unforced ocean temperature changes in Atlantic and

Pacific tropical cyclogenesis regions, Proc. Natl. Acad. Sci., 103, 13905-13910, doi:10.1073/pnas.0602861103.

Sato, M., J. E. Hansen, M. P. McCormick, and J. B. Pollack (1993), Stratospheric aerosol optical depth, 1850-1990, J. Geophys. Res. 98, 22987-22994.

Singh, O. P., T. M. A., Khan, S. Rahman (2000), Changes in the frequency of tropical cyclones over the North Indian Ocean, Meteorol. Atmos. Phys., 75, 11-20.

Song, Y., and W. A. Robinson (2004), Dynamical mechanisms for stratospheric influences on the troposphere, J. Atmos. Sci., 61, 1711-1725.

Swanson, K. L. (2008), Nonlocality of tropical cyclone intensities, Geochem. Geophys. Geosyst.,9,Q04V01, doi:10.1029/2007GC001844.

Tang, B.H., and J. D. Neelin (2004), ENSO Influence on Atlantic hurricanes via tropospheric warming, Geophys. Ress Lett, 31, L24204.

Ting, M., S. Camargo, C. Li, and Y. Ushnir (2015), Natural and Forced North Atlantic Hurricane Potential Intensity Change in CMIP5 Models, J. Clim., 28, 3926-3942.

Tippett, M. K., S. J. Camargo, A. H. Sobel (2011), A Poisson Regression Index for Tropical Cyclone Genesis and the Role of Large-Scale Vorticity in Genesis, J. Clim, 24, 2335-2357, DOI: 10.1175/2010JCLI3811.1.

Trenberth, K. E., and D. J. Shea (2006), Atlantic hurricanes and natural variability in 2005, Geophys. Res. Lett., 33, L12704, doi:10.1029/2006GL026894. J. Clim, 24, 2335-2357,

Uppala, S. M., P. W. Kållberg, A. J. Simmons, U. Andrae, V. da Costa Bechtold, M. Fiorino, J. K. Gibson, J. Haseler, A. Hernandez, G. A. Kelly, X. Li, K. Onogi, S. Saarinen, N. Sokka, R. P. Allan, E. Andersson, K. Arpe, M. A. Balmaseda, A. C. M. Beljaars, L. van de Berg, J. Bidlot, N. Bormann, S. Caires, F. Chevallier, A. Dethof, M. Dragosavac, M. Fisher, M. Fuentes, S. Hagemann, E. Hólm, B. J. Hoskins, L. Isaksen, P. A. E. M. Janssen, R. Jenne, A. P. McNally, J.-F. Mahfouf, J.-J. Morcrette, N. A. Rayner, R. W.

Saunders, P. Simon, A. Sterl, K. E. Trenberth, A. Untch, D. Vasiljevic, P. Viterbo, and J. Woollen (2005), The ERA-40 re-analysis, Q.J.R. Meteorol. Soc., 131, 2961-3012.

Vasquez, T. (1994), Weather forecasting handbook. Weather Graphics Technologies, 112, 154-155.

Vimont, D. J., and J. Kossin (2007), The Atlantic Meridional Mode and hurricane activity, J. Res. Lett., 34, 7709, doi:10.1029/2007GL029683.

Vecchi, G. A., and B. J. Soden (2007), Effect of remote sea surface temperature change on tropical cyclone potential intensity, Nature, 450, 1066-1070, doi:10.1038/nature06423.

Vecchi, G. A., S. Fueglistaler, I. M. Held, T. R. Knutson, and M. Zhao (2013), Impacts of atmospheric temperature trends on tropical cyclone activity, J.Climate, 26, 3877–3891, doi:10.1175/JCLI-D-12-00503.1.

Wang, B., and J. C. L. Chan (2002), How strong ENSO events affect tropical storm activity over the western north Pacific, J. Clim, 15, 1643-1658.

Wang, C., and S. K. Lee (2009), Co-variability of tropical cyclones in the North Atlantic and the eastern North Pacific, Geophys. Res. Lett., 36, L24702, doi:10.1029/2009GL041469.

Wang, C., S. Dong, A. T. Evan, G. R. Foltz, and S.-Ki Lee (2012), Multidecadal Covariability of North Atlantic Sea Surface Temperature, African Dust, Sahel Rainfall, and Atlantic Hurricanes, J. Climate, 25, 5404–5415, doi: http://dx.doi.org/10.1175/JCLI-D-11-00413.1.

Wang, S., S. J. Camargo, A. H. Sobel, and L. M. Polvani (2014), Impact of the Tropopause Temperature on the Intensity of Tropical Cyclones: An Idealized Study Using a Mesoscale Model, J. Atmos. Sci., 71, 4333-4348, DOI: 10.1175/JAS-D-14-0029.1.

Wang, H., L. Long, A. Kumar, W. Wang, J.-K.E. Schemm, M. Zhao, G.A. Vecchi, T.E. LaRow, Y.-K. Lim, S.D. Schubert, D.A. Shaevitz, S.J. Camargo, N. Henderson, D.Y. Kim, J.A. Jonas, and K.J.E. Walsh (2014), How well do global climate models simulate

the variability of Atlantic tropical cyclones associated with ENSO?, J. Climate, 27, no. 15, 5673-5692, doi:10.1175/JCLI-D-13-00625.1.

Wang, Y., K.-H. Lee, Y. Lin, M. Levy, and Renyi Zhang (2014), Distinct effects of anthropogenic aerosols on tropical cyclones, Nature Climate Change, 4, 368-373, doi:10.1038/nclimate2144.

Wolter, K., and M. S. Timlin (2011), El Nino/Southern Oscillation behaviour since 1871 as diagnosed in an extended multivariate ENSO index (MEI.ext), Int. J. Climatol. 31 1074–87.

Wu, L., C. Chou, C.-T. Heng, R. Huang, T. R. Knutson, J. J. Sirutis, S. T. Garner, C. Kerr, C.-J. Lee, and Y.-C. Feng (2014), Simulations of the present and late 21st century western North Pacific tropical cyclone activity using a regional model, J. Clim., 27(9), DOI:10.1175/JCLI-D-12-00830.1.

Zhang, R., and T. L. Delworth (2006), Impact of the Atlantic multidecadal oscillations on India/Sahel rainfall and Atlantic hurricanes, Geophys. Res. Lett., 33, L17712, doi: 10.1029/2006GL026267.

Zhang, R., T. L. Delworth, R. Sutton, D. L. R Hodson, K. W. Dixon, I. M. Held, Y. Kushnir, J. Marshall, Y. Ming, R. Msadek, J. Robson, A. J. Rosati, M. Ting, G. A. Vecchi (2013), Have Aerosols Caused the Observed Atlantic Multidecadal Variability?, J. Atmos. Sci., 70(4), DOI:10.1175/JAS-D-12-0331.1.

Zhang, W., W. Perrie, and W. Li (2006), Impacts of Waves and Sea Spray on Midlatitude Storm Structure and Intensity, Mon. Wea. Rev., 134, 2418-2442.

Zhao, M., I. M. Held, S. J. Lin, and G. A. Vecchi (2009), Simulations of global hurricane climatology, interannual variability, and response to global warming using a 50km resolution GCM, J. Clim., 22(24), DOI:10.1175/2009JCLI3049.1.

Table 1. Tropical cyclone development domains and season of activity. See also Figure 1.

Basin	Coordinates	Main Season
East Pacific (EP)	180-270 ºW, 10-20 ºN	Jun-Nov
North Atlantic (NA)	300-340 ºW, 10-20 ºN	Jun-Nov
North Indian (NI)	60-90 ºE, 10-20 ºN	Apr-Dec
South Indian (SI)	45-120 ºE, -10-20) ºS	Nov-Apr
South Pacific (SP)	150 ºE - 210 ºW, -10-20) ºS	Nov-Apr
West Pacific (WP)	110-150 ºE, 10-20 ºN	Jun-Nov

Table 2. List of all variables in this study, including their source and time period. The abbreviations: E, M, and N represent ERA-Interim, MERRA, and NCEP/NCAR, respectively. The resolutions for the ERA-Interim, MERRA, and NCEP/NCAR are, respectively: 80 km, 1/2° × 2/3°, and 2.5° × 2.5°. The stratospheric AOD is computed as zonal means over 8º latitude bands, ranging from 90°N to 90°S.

Variable	Abbreviation	Source	Time Period
1. SST	SST	E/M/N	1980-2009
2. SST-100 hPa Temperature	SST-100	E/M/N	1980-2009
3. 100 hPa Temperature	T at 100	E/M/N	1979-2009
4. Relative SST (SST (basin - tropics))	Rel. SST	E/M/N	1979-2009
5. Wind shear (u 200 – u 850 hPa)	Wind Shear	E/M/N	1980-2009
6. Mid-troposphere relative humidity (700-500 hPa)	RH (700-500)	E/M/N	1980-2009
7. Lower troposphere relative humidity (1000-850 hPa)	RH (1000-850)	E/M/N	1980-2009
8. Precipitable water	Precip. Water	E/M/N	1980-2009
9. Black carbon AOD	BC AOD	GOCART	1980-2009
10. Organic carbon AOD	OC AOD	GOCART	1980-2009
11. Dust AOD	DU AOD	GOCART	1980-2009
12. Sea salt AOD	SS AOD	GOCART	1980-2009
13. Sulfate AOD	SU AOD	GOCART	1980-2009
14. Stratospheric AOD	SAOD	NASA	1980-2009
15. ENSO Index	ENSO	NOAA	1980-2009
16. NAO Index	NAO	NOAA	1980-2009
17. QBO Index	QBO	NOAA	1980-2009
18. AMM Index	AMM	NOAA	1980-2009

Table 3. Climate models from the Coupled Model Intercomparison Project Phase 5 (CMIP5) used in the multi-model mean comparison for the 100 hPa temperature.

Climate Model	Institution	Time Period	Resolution (^{o}lat × ^{o}lon)
CCSM4	National Center for Atmospheric Research	1950-2005	0.94 x 1.25
CNRM-CM5	National Centre for Meteorological Research	1950-2005	1.41 x 1.41
GFDL-CM3	NOAA Geophysics Dynamics Laboratory	1950-2005	2.0 x 2.5
GISS-E2-R	NASA Goddard Institute for Space Studies	1950-2005	2.0 x 2.5
NorESM1-M	Norwegian Meteorological Institute	1950-2005	1.88 x 2.5

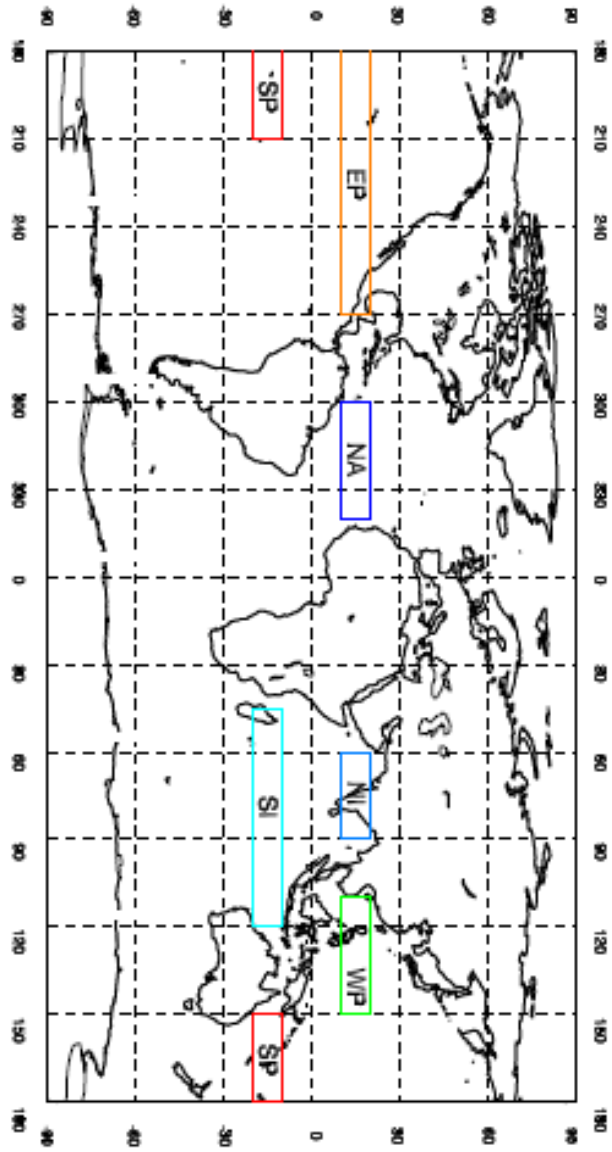

Figure 1. Global map of tropical cyclone development regions: East Pacific (EP), North Atlantic (NA), North Indian (NI), West Pacific (WP), South Pacific (SP), and South Indian (SI). Note that no land grid boxes are considered in the above domains. See also Table 1.

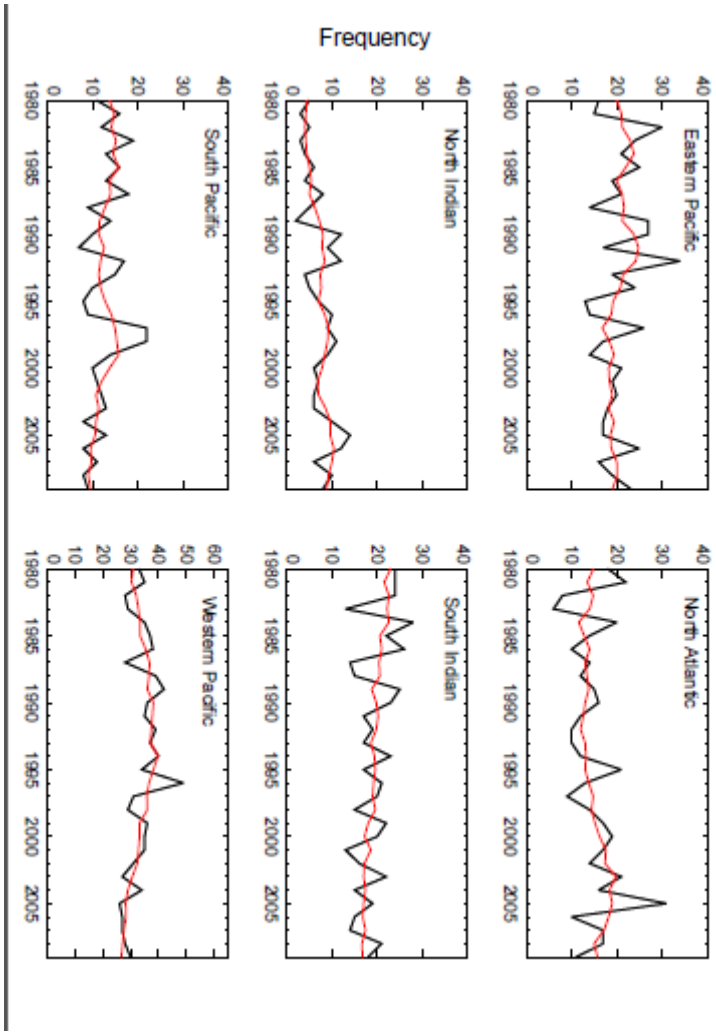

Figure 2. Seasonal tropical storm frequency in the oceanic basins of the East Pacific, North Atlantic, North Indian, South Indian, South Pacific, and Western Pacific. The black lines represent the annually averaged seasonal storm frequency. The red line shows a 5-year running mean.

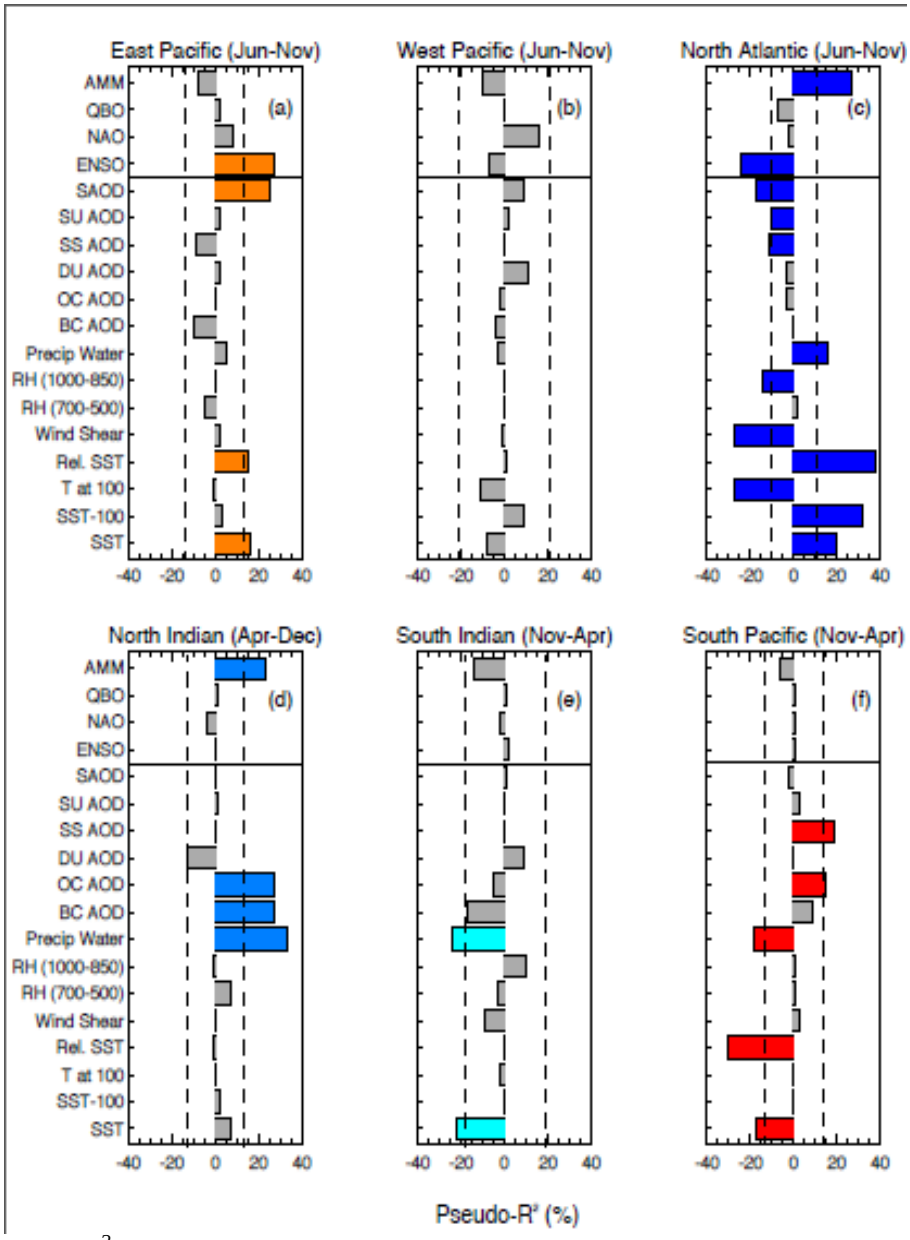

Figure 3. Pseudo-R^2 for Poisson regression models for the TC frequency with each of the 18 variables listed in Table 2 as an explaining variable. Data for the explaining variables are taken from the Modern-Era Retrospective Analysis for Research and Applications (MERRA) in the seasons as defined in Table 1. The results are shown for the tropical cyclone development region of the (a) East Pacific, (b) West Pacific, (c) North Atlantic, (d) North Indian, (e) South Indian, and (f) South Pacific. If the sign of the regression coefficient is negative for a particular variable, the value of pseudo-R^2 for that variable is multiplied by -1 to display negative bars. The variables are tested for significance at the 2.5% level using a chi-squared distribution. Non-significant variables are in grey. Variables above the solid horizontal line represent dynamical variables while those below represent thermodynamical variables.

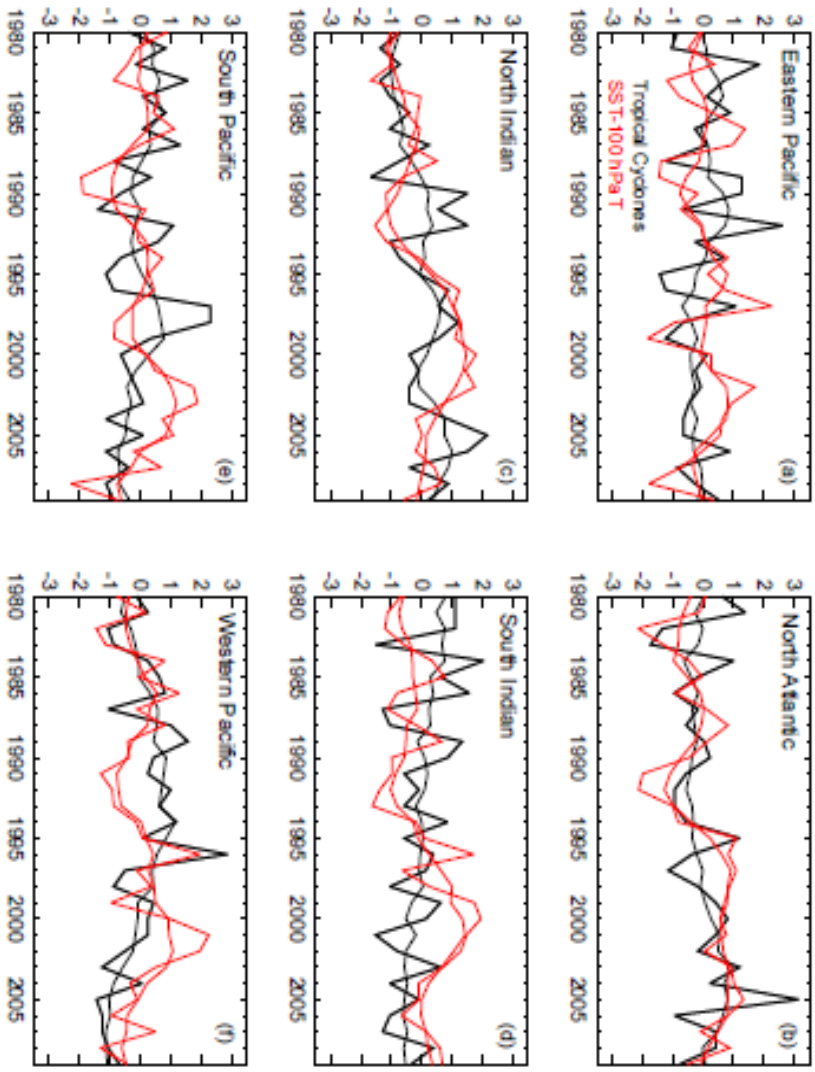

Figure 4. Normalized time series of tropical storm frequency and seasonal mean temperature gradient between the SSTs and 100 hPa from the Modern-Era Retrospective Analysis for Research and Applications (MERRA) dataset. The panels correspond to: (a) East Pacific, (b) North Atlantic, (c) North Indian, (d) South Indian, (e) South Pacific, and (f) Western Pacific. The black lines represent tropical cyclone frequency and the red lines are the SST-100 hPa temperatures.

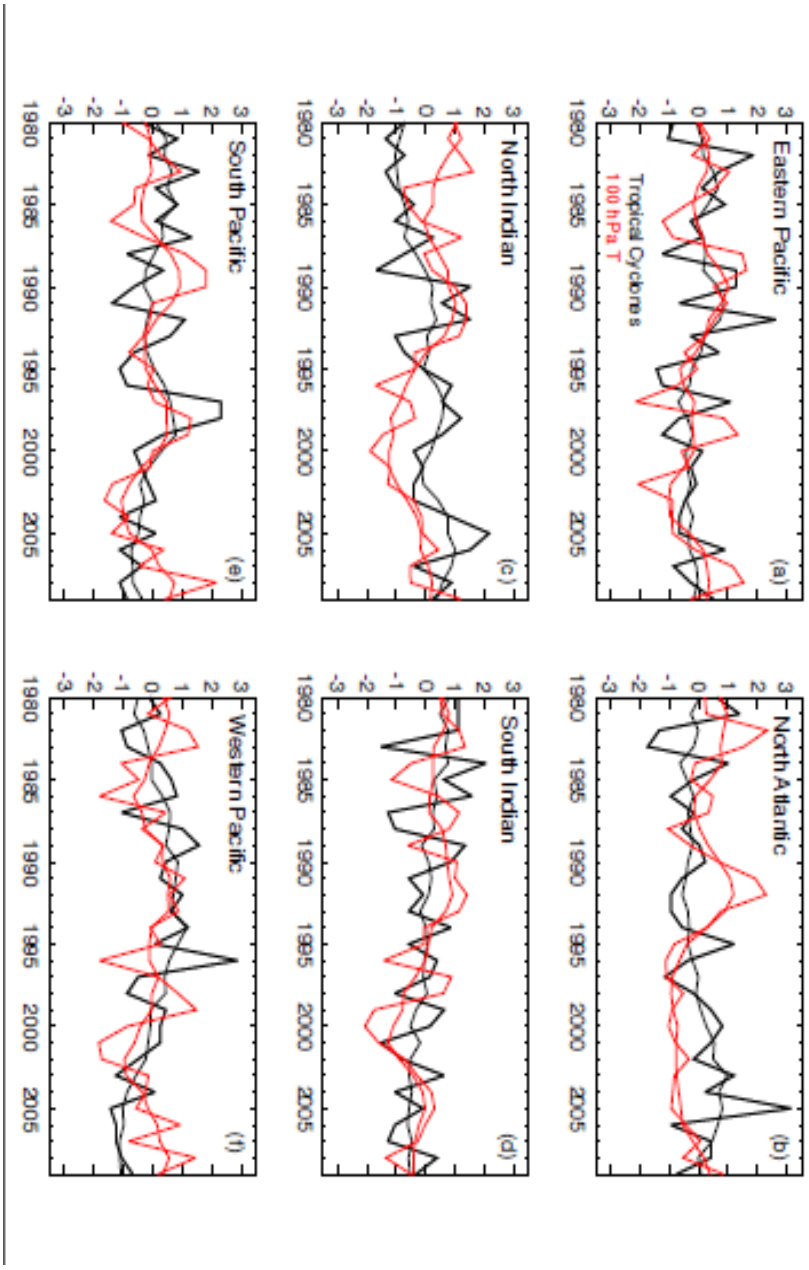

Figure 5. Same as Figure 4 but for seasonal mean temperatures at 100 hPa.

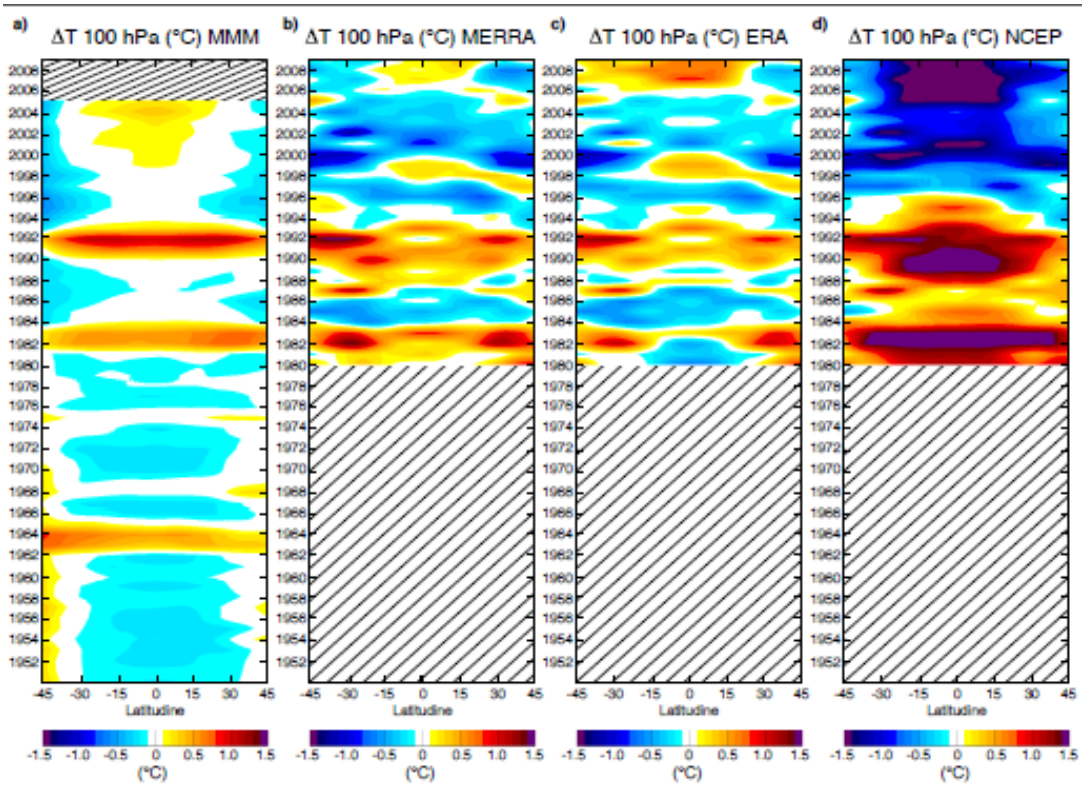

Figure 6. Zonally averaged lower stratospheric temperature anomalies at 100 hPa for (a) the Coupled Model Intercomparison Project Phase 5 (CMIP5) multi-model mean (MMM); (b) the Modern-Era Retrospective Analysis for Research and Applications (MERRA); (c) the European Centre for Medium-Range Weather Forecasts (ECMWF) Reanalysis (ERA-Interim); and (d) the National Centers for Environmental Prediction (NCEP). The MMM covers the period 1950-2005; the reanalyses cover the period 1980-2009. The values are averaged over the regions and seasons of main tropical cyclone development as listed in Table 1.

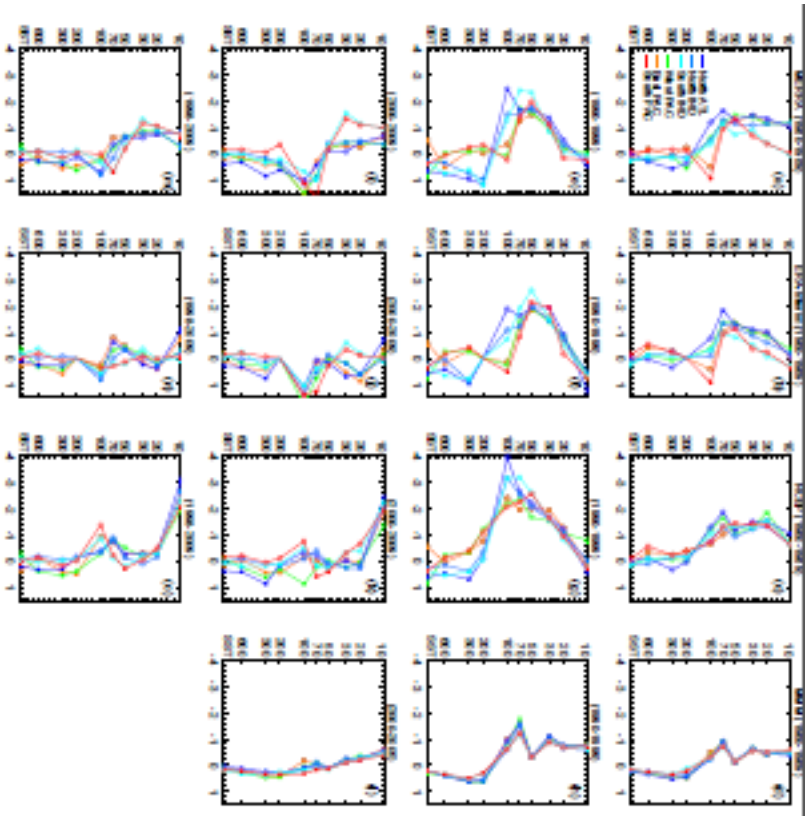

Figure 7. Vertical distribution of temperature trends over the periods (a-d) 1980-1989, (e-h) 1990-1999 , (i-k) 2000-2009, (l) 2000-2005, and (m-o) 1998-2009 from (first three columns from the left) the Modern-Era Retrospective Analysis for Research and Applications (MERRA), the European Centre for Medium-Range Weather Forecasts (ECMWF) Reanalysis (ERA-Interim), the National Centers for Environmental Prediction (NCEP), and (right panel) the multi-model mean (MMM) from the Coupled Model Intercomparison Project Phase 5 (CMIP5) models. The values are averaged over the regions and seasons of main tropical cyclone development, as listed in Table 1. The lowest level represents actual sea surface temperature (SST). Statistical significance at the 95% level is indicated by a closed circle and non-significance by an open circle.

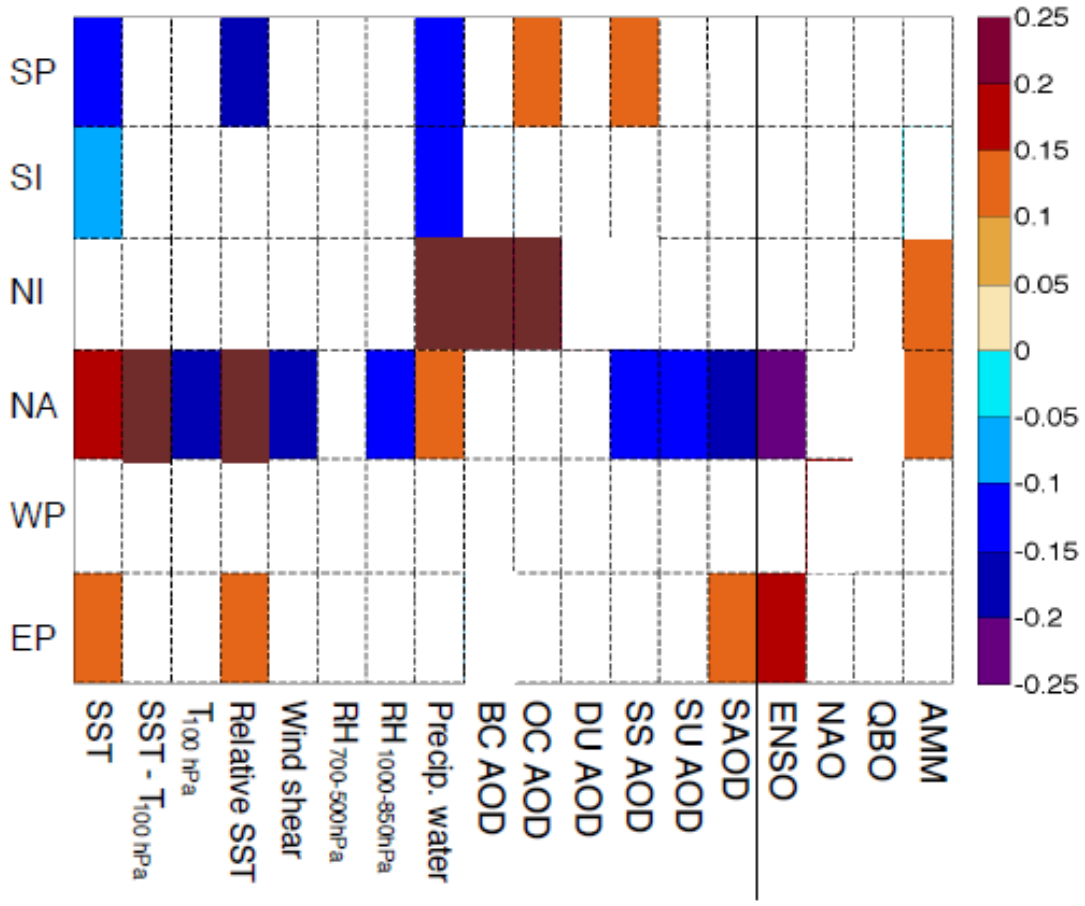

Figure 8. Map of regression coefficients, or the change in the logarithm of the mean of the tropical cyclone frequency per unit of change in the meteorological parameters, aerosol optical depth (AOD), and circulation indices in the domains listed in Table 1. Filled boxes denote statistical significance at the 2.5% significance level. Non-significant values are indicated by white boxes. The solid horizontal lines separate thermodynamic (left) and dynamic (right) variables.

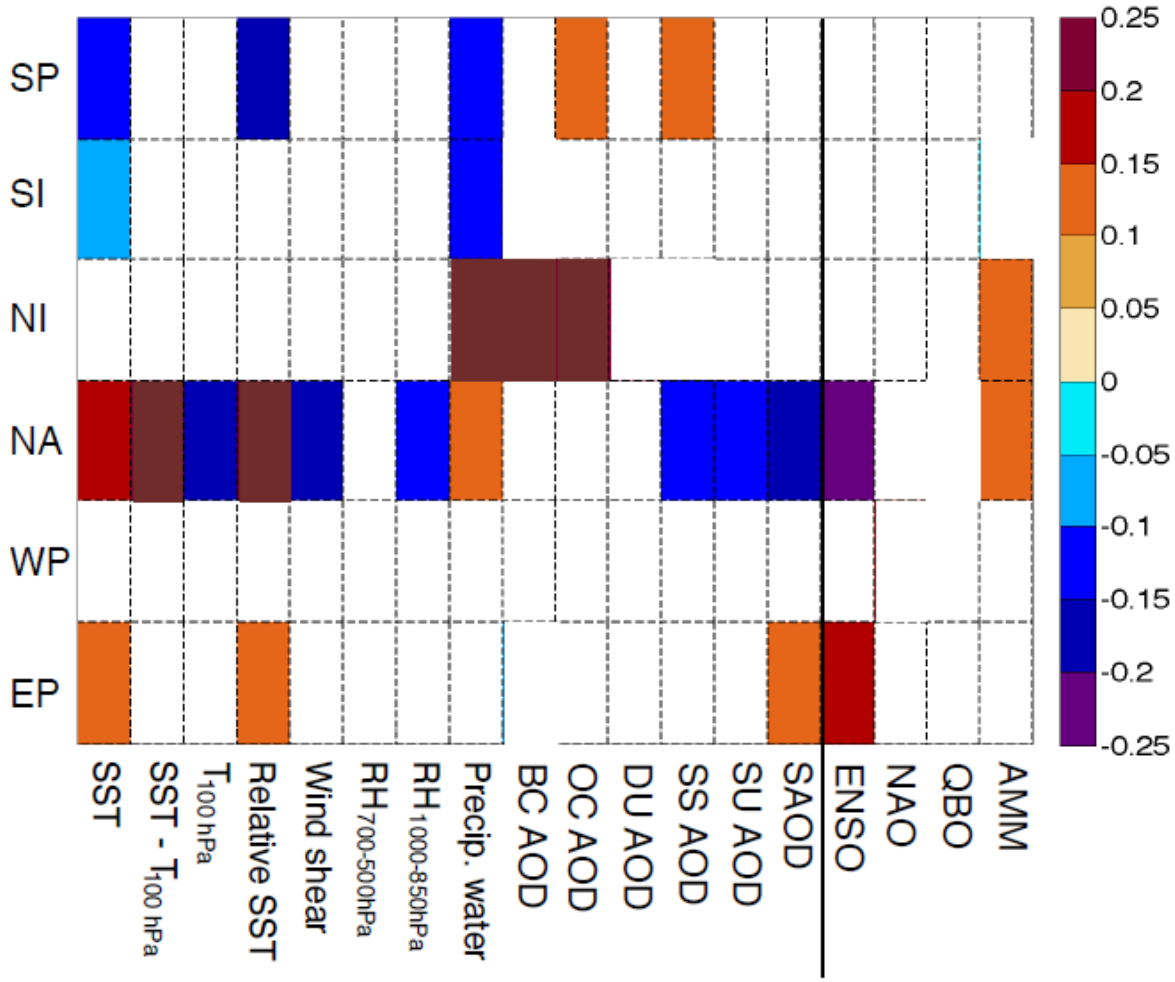

Figure 9. Comparison of pseudo-R^2 values, as defined in Figure 3, but with the first 8 variables as listed in Table 2 as an explaining variable. The results are shown for the tropical cyclone development region of the (a) East Pacific, (b) West Pacific, (c) North Atlantic, (d) North Indian, (e) South Indian, and (f) South Pacific.